We are IntechOpen, the world's leading publisher of Open Access books Built by scientists, for scientists

4,800
Open access books available

122,000
International authors and editors

135M
Downloads

Our authors are among the

154
Countries delivered to

TOP 1%
most cited scientists

12.2%
Contributors from top 500 universities

CLARIVATE ANALYTICS BOOK CITATION INDEX INDEXED

WEB OF SCIENCE™

Selection of our books indexed in the Book Citation Index in Web of Science™ Core Collection (BKCI)

Interested in publishing with us?
Contact book.department@intechopen.com

Numbers displayed above are based on latest data collected.
For more information visit www.intechopen.com

8

Nanocomposites for Photovoltaic Energy Conversion

Xianwu Zeng and Yong X. Gan
Department of Mechanical, Industrial and Manufacturing Engineering
College of Engineering, University of Toledo, Toledo, OH 43606,
USA

1. Induction

1.1 Composite materials

A composite is a multiphase solid material. It is incorporated by two or more individual materials through physical or chemical methods. The performance of different materials to complement each other will produce synergistic effects (Ivanov et al., 2008; Lu et al., 2010). The overall property of composite materials is better than that of each original material to meet different requirements. These properties include mechanical, electrical, thermal, optical, electrochemical, catalytic behaviors etc. For example (Lu et al., 2010), investigating the synergistic effect of carbon nano-fiber (CNF) and carbon nano-paper on the shape recovery of shape memory polymer (SMP) composite shows that the combination of CNF and carbon nano-paper can improve the thermal and electrical conductivities of the SMP composite, which are much better than each of the components. The individual materials in a composite are referred to as two constituent materials. The two constituent materials are matrix and reinforcement. The matrix material is a frame to support the reinforcement material. So the reinforcement material can keep its relative position. The reinforcement is a functional material which can enhance the matrix properties. Composite metal matrix (substrates) includes aluminum, copper, titanium, magnesium and its alloys and non-metallic matrix includes synthesized resin, rubber, ceramics, graphite and carbon and so on. Reinforcement mainly includes glass fiber, carbon fiber, boron fiber , aramid fiber, silicon carbide fiber , asbestos fiber, whisker, metal wire and fine grain etc. In order to make use of synergistic effect to improve composite properties, optimum combination of matrix and reinforcement should be chosen.

1.2 Nanocomposites and their properties

A nanocomposite is a special composite where one of the phases has one, two or three dimensions less than 100 nanometers (nm, 10^{-9} m). A nanocomposite also includes the material where the structures between the different phases that make up the material are in nano-scale (Beecroft & Ober, 1997). In the broadest sense, nanocomposites can also include porous media, colloids, gels and polymers, because in these materials the particles or structures are in nano scale. One nanometer is equivalent to the length to tightly line up

10~100 atoms. Nano-materials include nano-powders, nano-fibers, nano-particles and nano-thin films. Their structures are between atom (molecular) size and macro size. Materials in nano-scale have special effects such as quantum size effect, surface effect, small-size effect and macroscopic quantum tunneling effect etc.

Quantum size effect

Quantum size effect is one of the fundamental physical properties of nano-particles. When the particle size decreases to a nano-scale, the electronic energy levels of the particle atom become discrete and the energy gap becomes wider. This phenomenon is called quantum size effect. This effect does not come into play when the particles are in micro dimensions. However, quantum effects become dominant when the particles sizes decrease to nanometer, especially when the dimensions are in 100 nanometers or less. So the nanometer size dimension is also called quantum realm. The quantum size effect leads the nano-materials have very different magnetic, optical, acoustic, thermal, electrical and superconducting properties with conventional materials, such as very high non-linear optics, optical catalysis, high oxidability and reducibility etc. Due to quantum size effect, the galvanomagnetic and thermoelectric properties (electrical conductivity s, the Hall coefficient RH, charge carrier mobility m, and the Seebeck coefficient S) of nano-size PbSe thin film oscillate with the thin film thickness (3-200 nm) (Rogacheva et al., 2002). Silica glasses are doped with CdS and ZnS micro-crystals. Because of the quantum size effect, the optical absorption spectra and the photoluminescence spectra show that the optical absorption edges and the photoluminescence peaks shift to the higher energy side with decreasing the size of the micro-crystals (Zhao et al., 1994).

Surface effect

For a spherical particle, the ratio of surface area and volume is inversely proportional to the particle diameter. When particle size decreases to nano-scale, more atoms appear on surface relatively. For example, when particle diameter is 10 nm, the surface atom is about 20% of the total atoms; the diameter of 1 nm, the percentage of surface atoms increases to 99%. Almost all of the atoms are in surface. The particle surface becomes large relative the particle volume and the surface atoms are easy to combine with each other. This structure shows a high chemical activity. So, for the nano-materials, surface energy and surface binding energy are rapidly increasing compared to bulk particles. This change is called surface effect. For example, Au particles with dimension about 2 nm have no stable states; they change from octahedron, decahedron to icosahedron multicrystals. They are not liquid, not solid and can be called quasi-solid.

Small-size effect

When the particle size is close to or smaller than the light wavelength, the particle's de Broglie wavelength, semiconductor coherence length and the particle's penetration depth, the particle has new properties such as optical, thermal, acoustic, electrical, magnetic and mechanical properties etc. This phenomenon is the small size effect. For example, when the metal particle size is small than the light wavelength, the metal's color will become black. This means nano metal particles have very good light absorption and can be optothermal, photoelectrical materials. The melt temperature of bulk gold is 1064^0C, but 2 nm size gold particles melt temperature is only 327^0C. Nano-scale metal particles can be insulator.

Macroscopic quantum tunneling effect

Quantum tunneling refers to the phenomena of a particle's ability to penetrate energy barriers within electronic structures. Scanning tunneling microscope (STM) and Atomic force microscopy (AFM) are based on macroscopic tunneling effect.

1.3 Nanocomposite classification

Based on the matrix materials, the nanocomposites can be classified as ceramic-matrix nanocomposites, metal-matrix nanocomposites and polymer-matrix nanocomposites etc.

Ceramic-matrix nanocomposites

Ceramic materials such as oxides, nitrides, borides and silicides all can be the matrix of nanocomposites. Oxide ceramics include Al_2O_3, TiO_2, ZnO, $MgO \cdot Al_2O_3$, $3Al_2O_3 \cdot 2SiO_2$, PZT etc. Nitride ceramics include Si_3N_4, BN, AlN. Boride ceramics include CrB_2, ZrB_2 and TiB_2. Silicide ceramics include $MoSi_2$ etc. The reinforcement materials of ceramic-matrix nanocomposites are metals such as Fe, Al, Cu, Zn etc. Ceramic-matrix nanocomposites have very good optical, electrical and magnetic properties. Normally, preparing ceramic nanocomposite needs very high temperature. Some of the metallic components may easily react with the ceramic and thereby loses its metallic character. So, it should be careful in choosing immiscible metal and ceramic phases. There are also bi-phase ceramic/ceramic nanocomposites (Sternitzke, 1997). For example, low temperature nanocomposites Al_2O_3/SiO_2, SiO_2/MgO, Al_2O_3/TiO_2, AIN/BN; structure nanocomposites Al_2O_3/SiC, Si_3N_4/SiC, MgO/SiC etc.

Metal-matrix nanocomposites

Sometimes, or under special conditions, a metal can be the matrix of a nanocomposite. For example, Cu/Al_2O_3 metal matrix composite materials have both high strength and high conductivity. They can be used as electrodes and contact terminals. Here Cu is the matrix, and Al_2O_3 is the reinforcement. It has been identified that the Al_2O_3 particles in the consolidated composite material have the size smaller than 200 nm in diameter (Ying & Zhang, 2000).

Polymer-matrix nanocomposites

Polymers as the matrices of nanocomposites can enhance their performance, often in very dramatic degree. Nano-materials are the fillers, so, these materials are better described by the term nano-filled polymer composites. The fillers can be metals, metal oxides, polymers etc. This new class of composite materials has shown enhanced optical, electrical and dielectric properties. Polymer–inorganic nanocomposite materials are defined as inorganic nanofillers dispersed at a nanometer level in a polymer matrix. S.C. Tjong (Tjong, 2006) has reviewed polymer nanocomposites reinforced with respective layered silicates, ceramic nanoparticles and carbon nanotubes. The properties of nanocomposites depend not only on the properties of polymer matrices and nature of nanofillers but also on the way in which they are prepared. In order to achieve desired mechanical and physical characteristics, the nanofillers need disperse uniformly in the polymer matrices. Changli Lu et al (Lu et al, 2003) made ZnS–polymer nanocomposite films through chemical way. The ZnS nanoparticles were uniformly dispersed in the polymer matrix and the particles remained their original size 2.0–5.0 nm in diameter with a cubic phase structures. The resulting nanocomposite films have good thermal stability and exhibit excellent optical transparency in the visible region and higher refractive indices.

Nanocomposite materials are widely used in solar energy conversion. The application of solar cell is one of the most promising technologies in the last decade. Solar energy is clean and renewable. Converting solar energy into electricity provides a much-needed solution to the energy crisis the world is facing today. Solar cells convert sunlight into electricity based on photovoltaic effect. Even though the first generation and the second generation solar cells have become commercial products successfully, much research needs to continue to improve the energy conversion efficiency and reduce the cost of the products. Some of these efforts have produced materials that have shown very unique and important properties in contrast to traditional materials.

2. Sunlight and photovoltaic energy conversion

2.1 Sunlight and spectra

Almost all of the energy that drives the various systems (climate systems, ecosystems, hydrologic systems, etc.) found on the Earth originates from the sun. Solar energy is green power and renewable energy. Solar energy is abundant. Every day the sun radiates, or sends out, an enormous amount of energy to the earth, but only a little can be used. A sunlight or sunshine means the light radiates from the Sun and reaches to the earth. The sunlight contains energy. Based on quanta theory, the particle of light was given the name photon. A photon has an energy, E, proportional to its frequency v. This relation between the energy and frequency is called Planck relation or the Planck–Einstein equation:

$$E=hv \tag{2-1}$$

Since the frequency v, wavelength λ, and speed of light c are related by λv = c, the Planck relation can also be expressed as

$$E=\frac{hc}{\lambda} \tag{2-2}$$

Where h is Planck's constant (h= 6.626068×10^{-34} m^2 kg/s), c is the speed of light (c= 299,792,458 m/s). Because of the reflection of the aerosphere, about 70% energy within the light arrives at the earth and is absorbed by clouds, oceans and land masses. The sunlight is a kind of electro-magnetic wave or electromagnetic radiation. The spectrum of solar light is continuous. According to increasing order of wavelengths, the lights are ultraviolet, visible and infrared parts. The wavelengths are as follows:

Ultraviolet radiation (UV): 100-400 nm (not visible).

Visible light: 400-700 nm.

Infrared radiation (IR): 700 nm-1 mm (not visible)

On the contrary, the frequency decreases from ultraviolet, visible and infrared parts.
Figure 2.1 shows the solar radiation spectrum.
This figure shows the solar radiation spectrum for direct light at both the top of the Earth's atmosphere and at sea level. The Sun is like a blackbody and the surface temperature is about 5525 K (5250°C). The red part in the figure is the energy absorbed on sea level. Based Planck–Einstein theory, high frequency photon contains high energy. But in the sunlight the most parts are visible light and infrared radiation, only small part is ultraviolet light. Figure 2.1 shows that most of the energy is in visible and infrared spectrums. The solar energy

distribution according to wavelengths is visible light about 40%, infrared radiation about 50% and ultraviolet light about 10%.

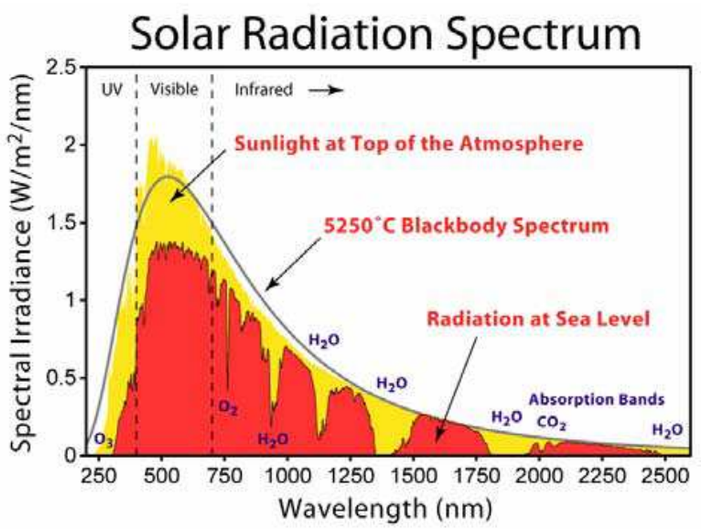

Fig. 2.1. Solar irradiance spectrum above atmosphere and at surface
Image created by Robert A. Rohde / Global Warming Art
(http://www.globalwarmingart.com/wiki/File:Solar_Spectrum_png)

2.2 Air mass

When the sunlight passes through the atmosphere, some of light will be absorbed by the air and dust. This means part of the light power will be lost. The Air Mass quantifies the power reduction when the light passes through the atmosphere. It is defined as:

$$AM=\frac{1}{\cos(\theta)} \tag{2-3}$$

where θ is the angle from the vertical direction (Figure 2.2). When the sun is directly overhead, the Air Mass is 1 (θ=90°).

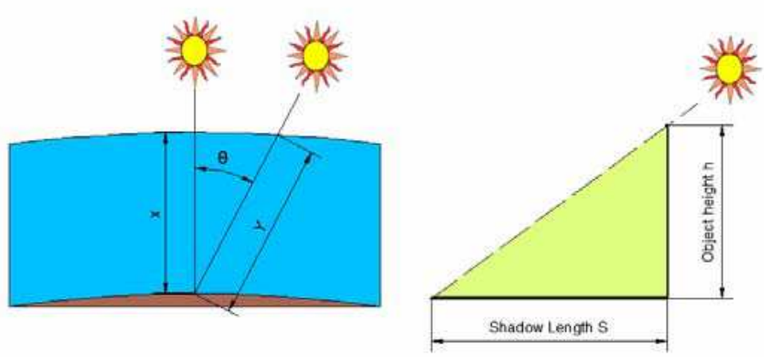

Fig. 2.2. AM measurement

The measurement of AM is in Figure 2.2. Here h is the object height, s is the shadow length. From the geometry, the AM can be calculated:

$$AM=\frac{1}{\cos\theta}=\sqrt{1+\left(\frac{s}{h}\right)^2} \quad (2\text{-}4)$$

The above formula is an ideal condition that assumes the atmosphere is a flat horizontal layer, but the Earth is a sphere and the atmosphere is like sphere shell. An equation which incorporates the curvature of the earth is:

$$AM=\frac{1}{\cos\theta+0.50572(96.07995-\theta)^{-1.6364}} \quad (2\text{-}5)$$

2.3 Standardised solar spectrum and solar irradiation

The power and the spectrum of the incident light can affect the efficiency of a solar cell. For measuring the solar cell efficiency, a standard spectrum and power density has been defined for both radiations outside the Earth's atmosphere and at the Earth's surface. AM0 is the standard spectrum outside the Earth's atmosphere, it is used for space cell. AM1.5G and AM1.5D are the standard spectrums at the Earth's surface. AM1.5G is for global and includes both direct and diffuse radiation. AM1.5D only includes direct radiation. Due to absorption (18%) and to scattering (10%) the intensity of AM1.5D radiation can be approximated by reducing the AM0 spectrum by 28%. The global spectrum is 10% higher than the direct spectrum. For the convenience of calculation, AM1.5G spectrum has been normalized to 1kW/m².

2.4 Photovoltaic energy conversion

The "photovoltaic effect" is the basic physical process through which a solar cell converts solar energy into electricity. Solar cell is actually a semiconductor diode. Sunlight is composed of photons, or "packets" of energy. These photons contain various amounts of energy corresponding to the different wavelengths of light. When photons strike a solar cell, they may be reflected or absorbed. When a photon is absorbed, the energy of the photon is transferred to thermal energy or electrical energy. The thermal energy can heat up the solar cell to a very high temperature and damage the solar cell. The absorbed energy can excite an electron in an atom of the cell. With its newfound energy, the electron is able to escape from its normal position associated with that atom to become part of the current in an electrical circuit. The absorbed energy of a photon is changed to thermal energy or electrical energy is related to the band-gap of the semiconductor material of the PV cell. A photon with energy equal to or greater than the band-gap of the materials is able to excite one electron when absorbed. If a photon with energy less than the band-gap all its energy will become thermal energy when absorbed. For the photons with more energy than the band-gap, the excess energy above the band-gap will also become thermal energy when absorbed. Because of this constraint, the efficiency of solar cell is very low. A good designed solar cell tries to absorb all the sunlight and change all the solar energy to electrical energy. This means the solar cell materials can be composites with different band-gap according to different sunlight photons energy.

Figure 2.3 shows photovoltaic current which is produced from semiconductor diodes. The diode connected with the current source represents the solar cell. I is the output current, and Ip is the photocurrent. Figure 2.3(a) shows the simplest solar cell model, where a diode and a current source are connected in parallel. It is noted that the source current (photocurrent)

is directly proportional to the solar radiation. The diode represents the p-n junction of a solar cell. The current (I) passes through the load is the difference between the photocurrent (Ip) and the current through the diode (I_D), and can be expressed by:

$$I=I_p-I_D=I_p-I_S\left[\exp\left(\frac{V}{mV_T}\right)-1\right] \tag{2-6}$$

In formula (2-6), m is the diode ideality factor, in the simplest cell m is represented by the ideal diode model, m=1. I_S is the reverse saturation current of a diode. I_S is in the order of 10^{-8} A/m^2. V_T is the thermal voltage of a diode. The relationship of the V_T and the temperature of the solar cell (T) can be shown in formula (2-7):

$$V_T=\frac{kT}{q} \tag{2-7}$$

where κ is the Boltzmann constant, and $k=1.38\times10^{-23}\left(\frac{J}{K}\right)$. q is the charge of electron, and $q=1.6\times10^{-19}(C)$.

Figure 2.3(b) shows a real solar cell circuit. There are serial (Rs) and parallel or shunt (R_{SH}) resistance in the equivalent circuit. The output current is

$$I=I_p-I_D-I_{SH}=I_p-I_S\left[\exp\left(\frac{V}{mV_T}\right)-1\right]-\frac{V+IRs}{R_{SH}} \tag{2-8}$$

where I_{SH} is the current passing through the shunt resistance and R_{SH} is the shunt resistance. Formula (2-8) is a transcendental equation, there is no analytical solution. But for an operating voltage V, the output current I can be determined numerically. In addition, the open circuit voltage, V_{OC}, can be calculated by setting I=0, i.e.

$$VOC\approx\frac{kT}{q}\ln\left(\frac{I_p}{I_S}-1\right) \tag{2-9}$$

In figure 2.3, short circuit current (I_{sc}) is the current when the terminals are connected to each other (zero load resistance). For a high-quality solar cell (low R_S, and high R_{SH}) the short-circuit current I_{SC} is

$$I_{SC}\approx I_p$$

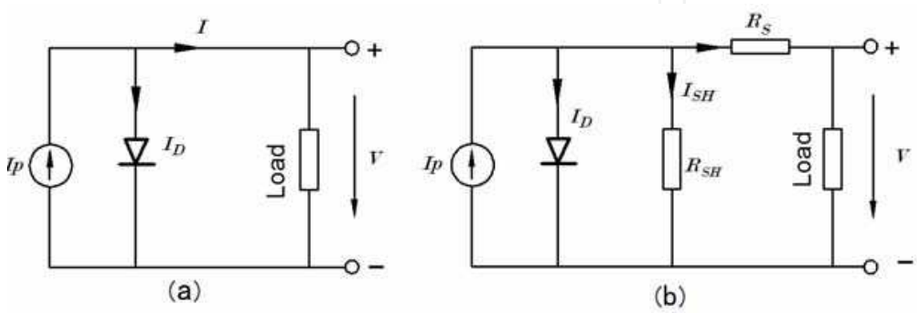

Fig. 2.3. The equivalent circuits of solar cell (a) Ideal model; (b) Practical model.

Current density

The values of I_S, R_S, and R_{SH} are dependent upon the physical size of the solar cell. In order to specify the properties of solar cell clearly, current density is introduced. It is the current produced per unit cell area:

$$J=J_p-J_S\left[\exp\left(\frac{V}{mV_T}\right)-1\right]-\frac{V+Jr_S}{r_{SH}} \tag{2-10}$$

where
J = current density (amperes/cm^2)
J_P = photogenerated current density (amperes/cm^2)
J_S = reverse saturation current density (amperes/cm^2)
r_S = specific series resistance (Ω-cm^2)
r_{SH} = specific shunt resistance (Ω-cm^2)

Efficiency η:

The power density is the product of voltage and current density.

$$P=J\,V \tag{2-11}$$

The maximum power density occurs somewhere between V = 0 (short circuit) and V = V_{oc} (open circuit) at a voltage V_m. The corresponding current density is J_m, and thus the maximum power density is $P_{d,m} = J_m V_m$. (Figure 2.4).
The efficiency of a solar cell is defined as the input power divided by the output power. If the incoming light has a power Ps, the efficiency will be:

$$\eta=\frac{P_{d,m}}{P_s} \tag{2-12}$$

FF is the solar cell fill factor.
It is defined as

$$FF=\frac{J_m V_m}{J_{SC} V_{OC}} \tag{2-13}$$

It gives a measure of how much of the open circuit voltage and short circuit current is "utilized" at maximum power (Figure 2.4). Using FF we can express the efficiency as:

$$\eta=\frac{J_{SC} V_{OC} FF}{P_S} \tag{2-14}$$

The four quantities J_{sc} (short circuit current density), V_{oc}, FF and η are frequently used to characterize the performance of a solar cell. They are often measured under standard lighting conditions, which implies Air Mass 1.5 spectrum, light flux of 1000W/m^2 and temperature of 25°C.
If shadows and defects present, they cause power loss because these areas become loads instead of generating power. The DC power may be converted to AC power by an inverter. The conventional energy causes pollution and greenhouse effect. Energy shortage is critical for most of the countries. These problems cause the demand for clean and renewable energy and lead to the significant expansion of the manufacture of solar cells. Currently available

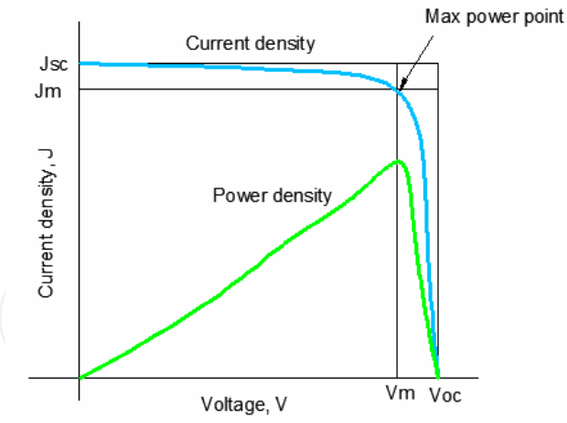

Fig. 2.4. The current-voltage and power-voltage characteristics of an ideal solar cell.

solar cells have the efficiencies about 6% (for the first generation silicon cells) to 40% (for the second and third generation multiple junction cells, Figure 2.5). It is estimated that over 8000 MW useful energy can be harvested over the world from sunlight each year with the 10% efficiency. But even now, the cost of photovoltaics is around $0.30/kWh, which is much higher than conventional power. The solar cell projects still need government support for the high cost. Only when the cost is close to that of the traditional power, the solar energy era will come.

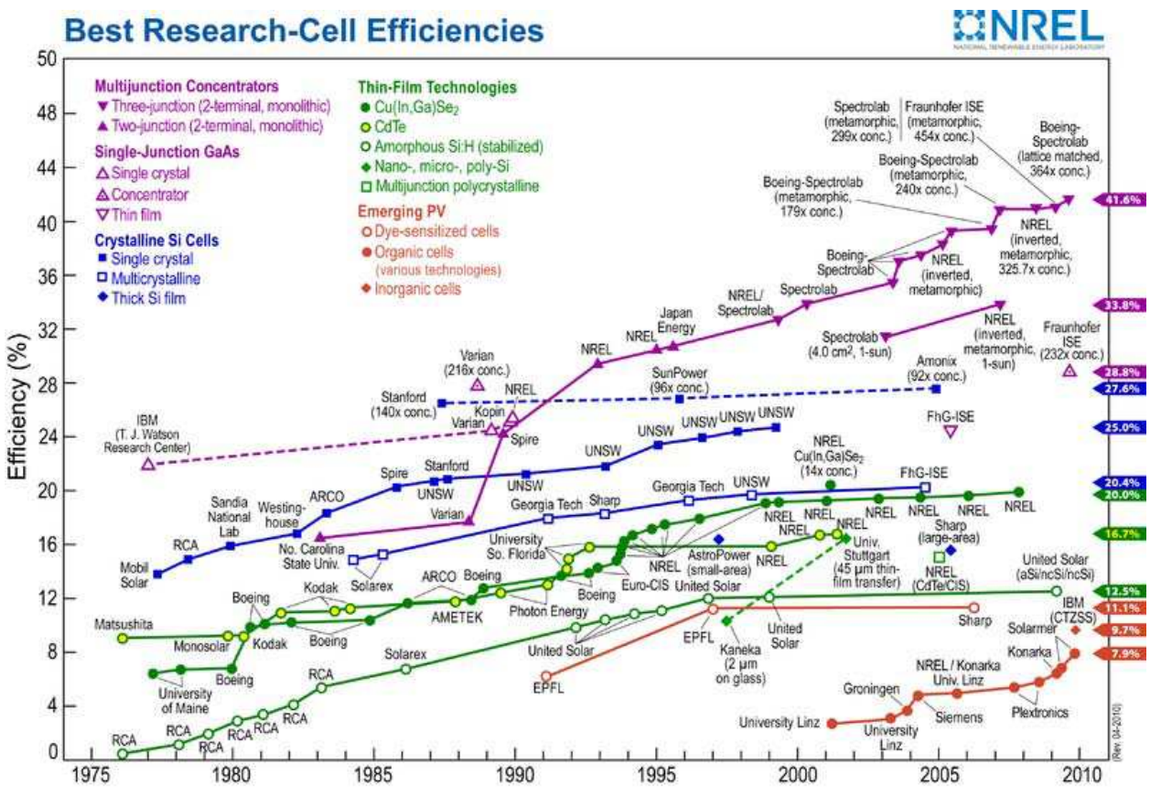

Fig. 2.5. NREL compilation of best research solar cell efficiencies
Chart courtesy of Larry Kazmerski, NREL

The National Renewable energy Lab (NREL) gives solar cell efficiencies based on different solar cell materials. Figure 2.5 shows the efficiencies of all kinds of solar cells and displays a very good prospect for all kinds of solar cells. Spectrolab (subsidiary of The Boeing Company) has set a new world record for terrestrial concentrator solar cell efficiency. The cell can convert 41.6% of concentrated sunlight into electricity. This is a multi-junction solar cell. This type of cell achieves a higher efficiency by capturing more of the solar spectrum. In a multi-junction cell, individual cells are made of layers, where each layer captures part of the sunlight passing through the cell. So this solar cell can absorb more energy from the sun's light (King, 2009). Table 2.1 gives the efficiencies description of the different solar cells in Figure 2.5.

Classification	Area cm^2	V_{OC} (V)	J_{SC} (mA/cm^2)	FF (%)	Efficiency (%)	Reference
GaInP/ GaInAs/ Ge	0.3174	3.192	1.696	88.74	41.6	(King, 2009)
Organic	0.0441	0.756	14.7	70.9	7.9	(Green et al., 2010)
CdTe	1.032	0.845	26.1	75.5	16.7	(Wu et al., 2001; Wu, 2004)
CIGS	0.419	0.69	35.5	81.2	19.9	(Repins et al., 2008)
Dye-Sensitized	0.219	0.736	20.9	72.2	11.1	(Chiba et al., 2006)

Table 2.1. Best efficiencies from Figure 2.5

First generation solar cell: single crystal silicon wafers (c-Si).

Because of broad spectral absorption range, Single crystal silicon solar cell can get high efficiency as 27.6% (Fig 2.5). The first generation photovoltaic cells are the dominant commercial products of solar cells taking more than 80% of the solar cell market. But the material processing and manufacturing are expensive.

Second generation: thin film

Based on thin film technology, the second generation solar cells also become commercial products. Thin film technology can reduce mass of material required for cell design, so it can reduce the cost for manufacturing solar cell. Normally, the efficiencies of thin-film solar cells are lower than the first generation solar cells. But thin film technology can make the solar cell panels on such substrates as light or flexible materials, even textiles. The second generation solar cells mainly include amorphous silicon (a-Si), polycrystalline silicon (poly-Si, not thin film), cadmium telluride (CdTe), copper indium gallium diselenide (CIGS) alloy etc. CdTe and CIGS are the mainly thin film solar cells on the market. The highest efficiencies of CdTe and CIGS can reach 16.5% and 19.9% respectively (Figure 2.5). Thin film solar cells are developing very fast. The market share is from about 10% (2007) to about 19% (2009).

Third generation and fourth generations:

The third generation solar cells include nanocrystal solar cells, photoelectrochemical (PEC) cells, polymer solar cells (thin film), dye sensitized solar cell (DSSC, thin film). The efficiency of the third generation is about 10%. The fourth generation cells are considered to be hybrid-inorganic crystals within a polymer matrix.

3. Nanocomposite manufacturing

In thin film soar cell, the basic manufacturing processing is the ability to deposit thin films of material. In this section, the main nano-manufacturing techniques for thin film solar cell will be introduced. These techniques include chemical bath deposition (CBD), close space sublimation (CSS), chemical vapor deposition (CVD), Magnetron sputtering and Electrodeposition (ED). There are many aspects should be considered for chose which process, such as cost, area size, in lab or in industry etc. The most important is the solar cell manufacturing technique includes a serial deposition processes. Each process has many possible choices. For example, making a CdS/CdTe solar cell includes transparent conductive oxides (TCO) deposition, buffer layer (CdS) deposition, absorber layer (CdTe) deposition and back contact deposition. CdTe layer can be deposited through one of CBD, CVD, CSS, mangnetron sputtering and electrodeposition. When one process is chosen, this process also affects the former (CdS) process and latter process (back contact), even the annealing process. The current status of technique for nanomanufacturing is discussed below.

3.1 Chemical bath deposition (CBD)

In 1933 Bruckman deposited PbS thin film by chemical bath deposition (CBD) or solution grown method. From then chemical bath deposition (CBD) has been used for decades to deposit thin films of various semiconductors (Hodes, 2003). The chemical bath deposition method is one of the cheapest methods to deposit thin films and nanomaterials. The CBD is very sample. It does not depend on expensive equipment and requires only solution containers and substrate mounting devices. CBD is a scalable technique that can be employed for large area batch processing or continuous deposition. The key advantages are low cost, large area, low temperature and atmospheric processing. With the development of thin film solar cell technology, CBD as the economical method is widely used in depositing buffer layers of CdS (and similar materials) in thin-film photovoltaic cells based on CdTe and $CuInSe_2$ (Mendoza-Perez et al., 2009; Ochoa-Landın et al., 2009; Lee, 2005; Castillo-Alvarado et al., 2010; Rose et al, 1999; Guillemoles et al., 2000; Hariskos et al., 2005; Romeo et al., 2004; Kylner, 1999; Shirakata et al., 2009; Noufi, 2006; Ennaoui et al., 2001). It takes advantage of the use of a reaction from a solution were different precursors can be dissolved easily. Depending on the deposition condition, the film growth can take place by ion–ion condensation or by adsorption of colloidal particles (cluster by cluster) from the solution onto substrates. Films deposited by this technique are proved to be of comparable quality with those produced by other sophisticated and expensive methods. There are some drawbacks of this method, such as the low material yield for film formation and the wastage of solution after every deposition which leads to treatment costs. Figure 3.1 shows the typical CBD devices.

Figure 3.1 shows the typical CBD-CdS devices in lab. The container is a beaker. Hot plate can heat the solution up to 90°C. The chemical solution contains Cadmium Acetate, Ammonium Acetate, Ammonium Hydroxide, and Thiourea. The chemical reaction results in the deposition of CdS onto all surfaces in the bath, including the surfaces of the ITO coated glass. Typically, for a 20-minute run, a thickness of 800-1000 Å can be achieved. The bath parameters such as concentration, bath temperature and deposition time greatly affect the morphology, thickness, refractive index, electrical resistivity, even the band gap of the deposited film (Lee, 2005; Contreras et al., 2002; Eze & Okeke, 1997; Marayanan et al., 1997). These properties of the buffer layer affect the performance of CdTe and CIGS solar cells.

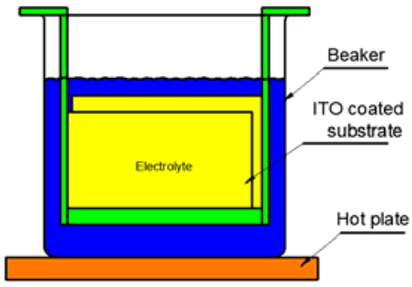

Fig. 3.1. Chemical bath deposition (CBD) devices for CdS in lab

3.2 Close space sublimation (CSS)

The close space sublimation (CSS) is widely used in CdS (and similar semiconductors) and CdTe thin film deposition in CdTe solar cells (Matsune et al., 2006; Kumazawa et al., 1997; Aramoto et al., 2003; Tsuji et al., 2000; Britta & Ferekides., 1993; Dzhafarov et al., 2005; Dobson et al., 2000; Enrıquez et al., 2007; Romeo et al., 2004; Khrypunov et al., 2006; Okamotoet al., 2000; Dhere et al., 1997; Ferekides et al., 2000). CSS is an attractive process and has many advantages. Compared with other deposition techniques, it can offer high deposition rate, it is able to produce films with large grains and can be easily scaled up for manufacturing purposes. CdTe CSS process is about 550-620°C, and CdS CSS process is about 500-600°C. The temperature is over CdTe and CdS recrystallization temperature, So, the grains size is larger than that with PVD or CVD process. CSS-CdTe grains size is about 290nm, PVD-CdTe giains size is 13nm (Moutinho et al., 2008).

Unlike other thin film deposition techniques, the distance between the source and the substrate is very short with millimeters or less, the source chosen is very important, because the source strongly affects the control of the deposition parameters, especially the deposition rate (Pinheiro et al., 2006). The close space sublimation (CSS) technique is characterized by the short distance between the source and the substrate, which is usually less than 1 mm. Figure 3.2 shows the CSS system in lab.

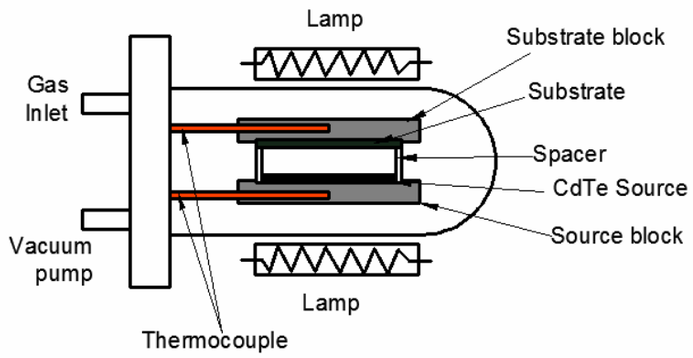

Fig. 3.2. CSS-CdTe deposition system

The CSS system is set up in a closed quartz chamber. When depositing films, the chamber can be filled a flow of gas from gas inlet. The gas can be hydrogen or inert gas such as Argon or Helium. O_2 is also found in CSS system. For example, CSS-CdS and CSS-CdTe deposition is in the ambient with O_2 (Ferekides et al., 2000). This was due to the fact that solar cells

fabricated with CdS films prepared in O_2 ambient exhibited higher efficiencies than devices fabricated with CdS films deposited in inert ambient. Some CSS systems also work under vacuum conditions of about 1 Torr.
The reactor consists of a source (CdS or CdTe) and a substrate, separated by quartz spacers. The source is in underside and the substrate is above. They are held by two graphite susceptors (blocks) respectively. Each graphite block is set one thermocouple to monitor the temperature of the source and the substrate. The aim of the CSS technique is to provide a temperature difference between the source and the substrate. This temperature difference enables a diffusion controlled transport mechanism.
Radiant heat from outside lamps can heat the graphite blocks and this heat then is transmitted to the source and the substrate. The heat can also be provided by the electrical current (resistance heating), using the two graphite blocks as resistances. A combination of the two can also be adopted.
In CSS system, the main parameters acting on the deposition rates are the spacing, the source and the substrate temperature, pressure and the ambient gas.

3.3 Chemical vapor deposition (CVD)

Chemical vapor deposition (CVD) is a chemical process used to produce high-purity, high-performance solid materials. In solar cell industry, CVD process is often used to produce semiconductor thin films such as SnO_2 (Wu et al., 2006), ZnO, CdS (Kumazawa et al., 1997) and CdTe (or similar semiconductors). In a typical CVD process, the sources (precursors) are volatile. When heated, they react/or decompose on the substrate surface to produce the desired deposit. Frequently, volatile by-products are also produced, which are removed by gas flow through the reaction chamber. Figure 3.3 shows the CVD system and process.

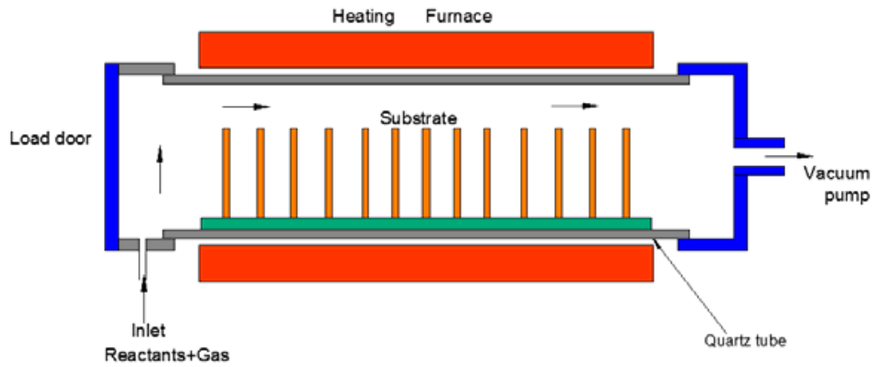

Fig. 3.3. CVD system and process

In this process, the substrate is placed inside a reactor to which reactants and inert dilute gases are supplied. The gaseous species move to the substrate and reactants are adsorbed onto the substrate with condenses. The gaseous by-products of the reactions are desorbed from the surface of the specimens and removed from the reaction chamber. The exhaust is subsequently trapped in a recycle tank through a vacuum pump. To precisely control the temperature at different locations in the chamber, multi-zone resistance heaters are used.
The deposition rate in a CVD process is controlled by the temperature. In high temperature range, mass-transfer controls the whole process of deposition. Nevertheless, in the low temperature range, the chemical reaction determines the rate of deposition. Transition between the two mechanisms is also found.

In thin film solar cell application, a number of forms of CVD are in wide use and are frequently referenced in the literature. The different types of CVD processes as follows:
According to pressure:

a. Atmospheric pressure CVD (APCVD) - CVD processes at atmospheric pressure
b. Low-pressure CVD (LPCVD) (Kumazawa et al., 1997; Rose et al., 1999)- CVD processes at subatmospheric pressures. Most modern CVD processes are either LPCVD or UHVCVD. The LPCVD process produces layers with excellent uniformity of thickness and material characteristics. The main problems with the process are the high deposition temperature (higher than 550°C) and the relatively slow deposition rate.
c. Ultrahigh vacuum CVD (UHVCVD) - CVD processes at a very low pressure, typically below 10^{-6} Pa (~10^{-8} torr).

Other methods:

PECVD—Plasma-Enhanced CVD; CVD processes that utilize plasma to enhance chemical reaction rates of the precursors. PECVD processing allows deposition at lower temperatures, which is often critical in the manufacture of semiconductors.
ALCVD—Atomic layer CVD (Naghavi et al., 2003); It is based on the sequential use of a gas phase chemical process. The majority of ALD reactions use two chemicals (precursors). These precursors react with a surface one-at-a-time in a sequential manner. By exposing the precursors to the growth surface repeatedly, a thin film is deposited.
MOCVD—Metalorganic chemical vapor deposition; CVD processes based on metal organic precursors. MOCVD is a common process for thin film solar cell deposition. It can be used on TCO, buffer layer and absorber layer, such as SnO_2 (Ferekides et al., 2000), CdS (Matsune et al., 2006; Kato et al., 2001; Tsuji et al., 2000), ZnO (Hariskos et al., 2005; Ennaoui et al., 2001) and CdTe (Sharma et al., 2003) etc.
There are also other type of CVD for different materials. The quality of the material varies from process to process, but in general, higher process temperature yields a material with higher quality and less defects.

3.4 Magnetron sputtering

Sputter deposition is a physical vapor deposition (PVD) method of depositing thin films by sputtering. In sputtering process, the material is released from the source at much lower temperature than evaporation. Figure 3.4 shows the sputter deposition process.

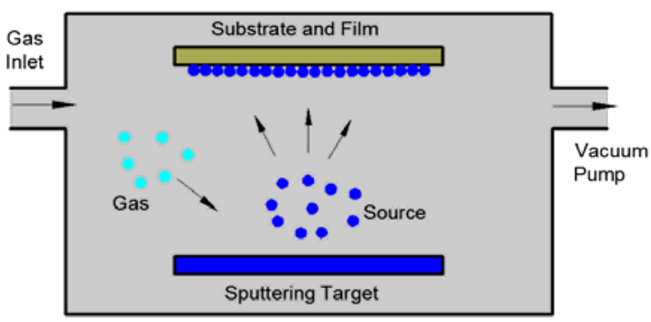

Fig. 3.4. Typical RF sputtering system.

The sputtering is ejecting material from a "target" (source), and then is deposited onto a "substrate". In figure 3.4, the substrate is placed the upside of a vacuum chamber with the

source material, named a target, underside. An inert gas (such as argon) is introduced at low pressure from gas inlet. The radio frequency (RF) power source causes the gas to become ionized. The ions are accelerated towards the target to bombard the atoms of the source material. The surface atoms are broken off from the target in vapor form and condense on the substrate surface to form thin film. The basic principle of sputtering is the same for all sputtering technologies. The sputtering is considered as a low temperature evaporation, which is realized by the ion bombardment of the target.

Normally the sputtering inert gas is argon. The principle for inert chosen is that the atomic weight of the sputtering gas should be close to the atomic weight of the target as for efficient momentum transfer. Neon is for sputtering light elements and krypton or xenon is for heavy elements. Reactive gases such as F_2, O_2, H_2 and N_2 etc can also be used to sputter compounds. The compound can be formed on the target surface, in-flight or on the substrate depending on the process parameters. The compounds have very good properties for application.

For example ZnTe:N is nitrogen-doped ZnTe. It can be the transparent back contact of a CdS/CdTe solar (Compaan et al., 2004). ZnTe:N films with ~750 nm thickness were deposited by reactive RF sputtering at ~350°C with 3% N_2 in the Ar sputter gas on aluminosilicate glass (Corning 1737). CdS:O (Wu, 2004) is CdS sputtered at room temperature in an oxygen/argon gas mixture. The CdS:O film has a higher optical bandgap (2.5–3.1 eV) than the poly-CdS film. The bandgap increases with an increase of oxygen content. A CdS thin film sputtered in a 2% oxygen/argon environment is still polycrystalline, but average grain size is around 3–5 nm, much smaller than the CdS film sputtered in an oxygen-free environment (~25 nm).

Sputtering is used extensively in the semiconductor industry to deposit thin films of various materials. For making efficient thin film photovoltaic (CdTe and CIGS) solar cells, sputtering is very useful technique.

In thin film CdTe solar cell, every layer can be deposited by sputtering including front contact transparent conductive oxide (TCO) (Wu et al., 2006; Wu et al., 2005; Romeo et al., 2010; Gupta et al., 2004; Santos-Cruz et al., 2006; Romeo et al., 2007; Tiwari et al., 2004; Lee, 2005; Romeo et al., 2003; Singh & McClure, 2003; Rose et al., 1999; Mitchell et al., 1977; Compaan et al., 2004; Wu, 2004; Colombo et al., 2009; Romeo et al., 2006; Minami, 2005; Singh et al., 1999;], buffer layer CdS (Wu et al., 2006; Wu et al., 2005; Romeo et al., 2010; Gupta et al., 2004; Lee, 2005; Romeo et al., 2003; Krishnan et al., 2009; Gupta et al., 2006; Compaan et al., 2004; Wu, 2004; Colombo et al., 2009; Singh et al., 1999), CdTe (Compaan et al., 2004; Gupta et al., 2004; Santos-Cruz et al., 2006; Mathew et al., 2004; Krishnan et al., 2009; Gupta et al., 2006; Compaan et al., 2004) and back contact (Compaan et al., 2004; Romeo et al., 2003; Fahrenbruch, 2007).

Xuanzhi Wu (Wu, 2004) introduced a kind of CdTe solar cell with a new structure and a new deposition process. In this structure, three layer of TCO film CTO, buffer layer ZTO, and window layer nano-CdS:O are deposited by RF sputtering in room temperature. RF sputtering is a mature technology with demonstrated production scalability. The new process has only one heat-up segment in the entire device fabrication process. The recrystallization of the first three layers and the interdiffusion at the three interfaces (CTO/ZTO, ZTO/CdS, and CdS/CdTe interfaces) are completed during CdTe deposition by the CSS technique. This process provides attractive alternatives for producing CdTe modules with a potential of high throughput and low cost by (1) increasing device efficiency up to 16.5%, (2) improving device yield,and (3) simplifying the device fabrication process.

Some researches made CdTe solar cell with all sputtering process. Gupta & Compaan (Gupta & Compaan, 2004) developed ZnO:Al/CdS/CdTe solar cell with all sputtering process. High temperature will make ZnO:Al degraded. This cell got efficiency as 14%. This result confirms that the moderate temperatures possible with magnetron sputtering can provide important advantages in cell fabrication and expand the range of materials available for thin- film polycrystalline solar cells. Marsillac et al (Marsillac et al., 2007) developed an Ultra-thin bifacial CdTe solar cell SnO2:F/CdS-/CdTe/ZnTe:N/ITO with all sputtering process. The efficiency can get over 5%.

In thin film CIGS solar cell, sputter is also a very common deposition process for thin film. Buffer layer (CdS or ZnO) and transparent conductive oxide (TCO, such as ITO, ZnO, ZnMgO and In_2S_3 etc) can be deposited by sputtering (Hariskos et al., 2005; Nakada & Mizutani, 2002;

Wuerz et al., 2009; Kylner, 1999; Romeo et al., 2004; Bhattacharya et al., 2001; Ennaoui et al., 2001; Ohashi et al., 2001; Delahoy et al., 2004; AbuShama et al., 2004; Contreras et al., 1999; Romeo et al., 2003). CIGS absorber layer also can be deposited by sputter. Zhang et al (Zhang et al., 2010) introduced a magnetron-sputtering process for CIGS absorber layer deposition. The deposition of CIGS films using CIGS quaternary-alloyed target is fabricated through sintering process. Cu2Se, In2Se3, and Ga2Se3 powders are used as raw materials. Selenium can be directly incorporated into absorbers from the sputtering of CIGS target. The results indicated that it is feasible to prepare CIGS absorbers with this method. Therefore, the selenization process that is difficult to control and perhaps use toxic H_2Se gas may be unnecessary.

Alan E. Delahoy et al (Delahoy et al., 2004) used hybrid process to form CIGS thin film. This hybrid process includes both thermal evaporation and sputtering. The linear source thermal evaporation supplied the In, Ga and Se, and the sputtering provided Cu. This hybrid process is applied to both stationary and moving glass substrates. The motivation for this work was the need to improve the ease and uniformity of Cu delivery. The hybrid process for CIGS formation shows good reproducibility, and shows promise for being manufacturable.

In the method of sputtering CIGS absorbers, a metal film of Cu, In, and Ga is sputtered at or near room temperature and reacted in a Se atmosphere at high temperature. This process has higher throughput than coevaporation and compositional uniformity can be more easily achieved. Dhere (Dhere, 2006) reviewed the CIGS layer deposition technique and introduced the reactive co-sputtering CIGS layer process. Co-sputtering Cu, In, Ga and Se together has the problem that Se can make the target insulated and prevents the accelerating ions to bombard the targets. The new reactive co-sputtering process is dual cylindrical magnetron sputtering from Cu–In–Ga targets in the presence of selenium vapor. In Cu-In-Ga sputtered cycle, each of the two targets becomes negatively biased alternatively. The sputtering takes place for a part of the cycle from one target and for the remainder of the cycle from the other target. This deposition process is efficient and can get appropriate Cu:In:Ga composition and allows the deposition of slightly Cu-poor, near-stoichiometric CIGS thin films.

Sputter deposition is a low temperature PVD process and evaporation is a high temperature process. Even the materials have very high melting points, they also can be easily deposited by sputtering. But for these materials with high melting points, evaporation is problematic or impossible. Sputter deposited films have a composition close to that of the source material. These films typically have a better adhesion on the substrate than evaporated

films. Sputtering process is in low temperature, this is compatible with reactive gases such as oxygen.
In sputtering process, the atoms can go anywhere after bombarded, which can lead to contamination problems. Also, active control for layer-by-layer growth is difficult compared to pulsed laser deposition and inert sputtering gases are built into the growing film as impurities.

3.5 Electrodeposition (ED)

Electrodeposition is also called electroplating. It is a plating process that uses electrical current to reduce cations of a desired material from a solution (electrolyte) and coat a conductive object with a thin layer of the material. Figure 3.5 shows a very simple electrodepostion device. The main components include DC voltage source, Anode, Cathode and electrolyte. There are additional devices such as heater and stirrer not shown here. In the electroplating process, the substrate is setup as cathode in the liquid solution (electrolyte). The electrolyte contains one or more dissolved metal salts as well as other ions that permit the flow of electricity. The Anode is a kind of metal. After added positive potential on the anode, the Anode metal atoms will be oxidized and dissolve in the solution. At the cathode, the dissolved metal ions in the electrolyte solution are reduced to atom and form a metal thin film on the cathode surface. The ions in the electrolyte bath are continuously replenished by the anode metal. This process is also called sacrificing anode method.

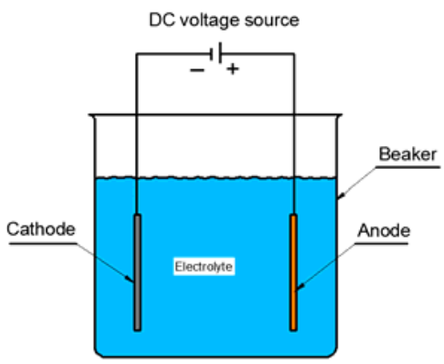

Fig. 3.5. Electrodeposition device in lab.

Metal thin films such as copper, molybdenum, gold and nickel etc can be deposited by electrodeposition process. The film thickness is in variations from nanosize to 100μm, which is controlled by the external electrical potential. In any process, the surface of the substrate must have an electrically conducting coating before the deposition can be done.
In thin film solar cells, such as CdTe, CIGS and DSSC solar cells, most of the thin film solar cell layers can be deposited by electrodeposition. For example, in a CdTe/PMeT structure solar cell (Gamboa et al., 1999), the CdTe absorber layer was deposited by electrodeposition process. In CdTe/ZnO structure solar cell, buffer layer ZnO was deposited on a conductive glass substrate by electrodeposition process (Levy-Clement et al., 2002). The glass was covered by a fluorine -doped tin dioxide ($F:SnO_2$) thin film.
Electroposition is quite slow process. Normally in CdS/CdTe solar cell, depositing a 2μm thin film of CdTe by electrodeposition process needs 2-3 hours. With a channel flow cell, this process was grown rapidly and the time can be cut to 20 min. The as-deposited films are

structurally more disordered, but after annealing and type-conversion they display superior electronic properties. The solar cell fabricated using a film prepared in the channel cell achieved efficiency 6% (Peter & Wang, 1999).

Electrodeposition is an economic, simple and successful method for preparing large area thin films. It is also a very convenient method for preparation of thin film CdTe on metallic (stainless steel) substrates (Mathew et al., 1999).

As a low cost process, electrodeposition is also widely used on CIGS solar cell thin film deposition. Kois et al (Kois et al., 2008) introduced a CIGS deposition process. Cu–In–Ga (CIG) layers of graded composition have been grown by one-step electrodeposition from thiocyanate complex electrolytes. Then the as-prepared CIG precursors are selenizated at Se-vapour to form CIGS thin film. In this process, the Ga-content in CIG films can be tailored by stirring in the process of simultaneous electrodeposition of Cu-In-Ga thin films.

Electrodeposition can be used in DSSC solar cell thin film deposition. In a ZnO/DSSC structure solar cell, electrodeposited nanoporous ZnO films exhibiting enhanced performance in dye-sensitized solar cells. Nanoporous ZnO films with grain size of 20–40 nm were grown by cathodic electrodeposition from an aqueous zinc nitrate solution. DSSCs were fabricated from nanoporous ZnO films and the cell performance could be greatly improved with the increase of ZnO film thickness. This kind of DSSC with double-layer ZnO films (8 μm thick nanoporous ZnO films on a 200 nm thick compact nanocrystalline ZnO film) achieved efficiency as high as 5.08% (Chen et al., 2006).

A counter electrode was prepared for a dye-sensitized solar cell (DSSC) through electrochemical deposition of mesoporous platinum can improve the performance of the solar cell. This kind of DSSC rendered a higher solar-to-electricity conversion efficiency of 7.6%, which is much higher than that of the sputter-deposited or most commonly-employed thermal deposited Pt counter electrodes (about 6.4%) (Yoon et al., 2008).

3.6 Other manufacture for thin film solar cell

There are still many process for thin film deposition such as close space vapor transport (CSVT) for CdTe thin film (Mendoza-Perez et al., 2009), physical vapor deposition (PVD)for CIGS thin film (Hermann et al., 2001) etc.

4. Nanocomposite application in thin film solar cell (Photovoltaic Cell)

A thin-film solar cell is made by depositing one or more thin layers (thin films) of photovoltaic materials on a substrate. The thickness of the thin-films is from a few nanometers to tens of micrometers. Thin film nano-composite solar cell materials include possible combinations of CdTe, TiO_2, CdS, $CuInS_2$, $CuInGaSe_2$ (CIGS), ZnS, ZnO, ZnTe, HgS, CuSCN, Ge, PbS etc. Some of them become commercial products, for example CdTe, $CuInGaSe_2$ (CIGS). However, most of them are still in lab research.

4.1 Solar cell structures

There are four basic structures for the photovoltaic solar cells, homojunction, heterojunction, p-i-n and n-i-p, multijunction.

Homojunction

Crystalline silicon solar cell is homojunction device. It is a simple P/N junction semiconductor. The free electrons and holes generated by light deep in the silicon diffuse to

the P/N junction, then separate to produce a current if the silicon is of sufficient high quality.

Heterojunction

Thin film solar cell such as CdTe and CIGS are heterojunction device. This device has two different semiconductors. For example, CIGS has two semiconductors as CdS and Cu(In, Ge)Se_2. The solar cell with this structure can absorb light much better than silicon. The two semiconductors layers have different roles. The top layer (CdS) is a "window" layer. This layer is transparent to light and allows almost all incident light to reach the bottom layer. The bottom layer is absorber which can generate electrons and holes when absorbs the sunlight. Figure 4.1 gives two kinds of heterojunction structure CdTe and CIGS solar cells (Romeo et al., 2004).

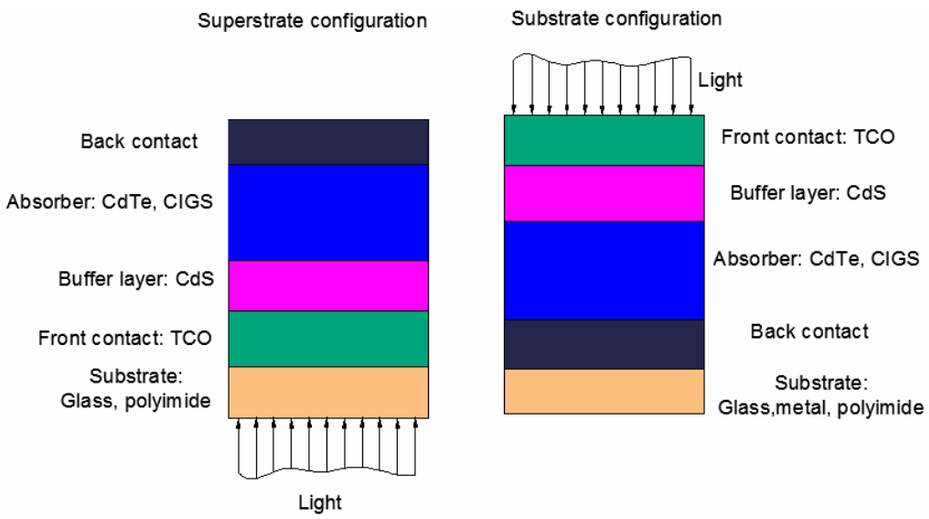

Fig. 4.1. Schematic cross-section of 'superstrate' and 'substrate' configurations for CdTe and CIGS solar cells

CdTe and CIGS have the same structures and compose 5 parts: substrate; front contact; buffer layer; absorber layer and back contact.

p-i-n/n-i-p Devices

Amorphous silicon thin-film cells are p-i-n structures. This structure has sandwiched three layers, p-type, i-type (intrinsic, undoped) and n-type layers. An electric field between the p- and n-type regions is set up which stretches across the middle intrinsic resistive region. The electric field can separate the free electrons and holes which generated by the incident light in the intrinsic region.

Multijunction Devices

Multijunction solar cells are called tandem cells. Normally, 2-junction or 3-junction solar cell is researched. This structure can achieve very high total conversion efficiency by capturing a larger portion of the solar spectrum. For example a 3-junction solar cell can achieve 41.6% efficiency (Figure 2.5). This cell is formed with individual cells and different band-gaps cells are stacked on top of one another. Each individual cell can capture one part of solar radiation. The band-gaps order is from top to bottom position with large to small band-gap. Most research in multijunction cells focuses on gallium arsenide cells.

4.2 CdS/CdTe thin film solar cell

CdS/CdTe thin-film solar cells have the potential to be mass-produced at low cost. Cadmium telluride (CdTe) has a band-gap of ~1.5 eV and the absorption spectrum is about 850nm. It is nearly ideal for sunlight absorption. So it has been recognized as a strong candidate for thin film solar cell applications. Cadmium telluride (CdTe) thin film solar cell is based on the use of cadmium telluride thin film, a semiconductor layer designed to absorb and convert sunlight into electricity. CdTe is a heterojunction p-type semiconductor. The cell was completed by adding top and bottom contacts. CdTe solar cells have very good optical property that one or two microns thickness thin film can absorb 98 percent of the sunlight. Although CdTe is most often used in PV devices without being alloyed, it is easily alloyed with zinc, mercury, and a few other elements to vary its properties. Many methods have been used for the fabrication of CdTe layers, for example close-spaced sublimation (CSS) (Chu et al., 1991; Kumazawa et al., 1997; Aramoto et al., 2003; Ferekides et al., 2000), electrodeposition (Gamboa et al., 1999), magnetron sputtering (Compaan et al., 2004; Gupta & Compaan, 2004), chemical vapor deposition (CVD) (Meyer & Saura., 1992), and metal-organic chemical vapor deposition (MOCVD) (Zoppi et al., 2006) and vapor phase epitaxy (VPE) (Levy-Clement et al., 2002).

CdS is one of the most crucial films, which serves as the window layer. Cell performance depends primarily on the electrical and optical properties of CdS film. The deep research shows the conversion efficiency of CdS/CdTe solar cells strongly depends on the ruggedness of the CdS surface (Tsuji et al., 2000). CdS is an n-type semiconductor. The optimum band gap is ~2.4 eV for solar spectrum and the direct band gap yields high optical absorption coefficient. CdS can be deposited by many methods such as CSS (Luschitz et al., 2009), MOCVD (Matsune et al., 2006; Tsuji et al., 2000), CVD (Kumazawa et al., 1997), magnetron sputtering (Gupta & Compaan., 2004), chemical bath deposition (CBD) and vacuum evaporation (Lee, 2005).

Much research has been performed on CdS/CdTe solar cells and very high energy conversion efficiencies have been achieved (Table 4.1).

J_{SC} (mA/cm^2)	V_{OC}(V)	F.F. (%)	Efficiency %	reference
23.6	0.814	73.25	14	(Compaan et al., 2004)
25.5	0.82	72	15.1	(Matsune et al., 2006)
25.36	0.826	72.2	15.12	(Kumazawa et al., 1997)
25.1	0.843	74.5	15.8	(Britta & Ferekides, 1993)
25.88	0.845	75.51	16.5	(Wu, 2004)

Table 4.1 High efficiencies CdS/CdTe solar cell parameters
(Measured under the standard condition: AM1.5, 100 mW/cm^2)

Morales-Acevedo (Morales-Acevedo, 2006) has made a physical analysis of the typical CdS-/CdTe superstrate solar cell. It shows that present record efficiencies are very close to the practical efficiency limit for a CdS/CdTe hetero-junction cell. The estimation of the maximum efficiency of hetero-junction CdS/CdTe solar cells is around 17.5%. The recorded highest efficiency is 16.5% (Wu, 2004), only 1% lower than the efficiency limitation. His work explains why the record efficiency for this kind of cells has been stable for the last 10 years, going up by less than 1% from 15.8% (Britta & Ferekides, 1993) to only 16.5%.

4.2.1 CdS/CdTe solar cell structure

Figure 4.2 gives the conventional structures of CdS/CdTe thin film solar cell. This structure has been developed over 30 years. Normally it has 5 parts:

1. Substrate-Glass or metal foil;
2. Front contact-Transparent conducting oxide (TCO);
3. CdS window layer;
4. CdTe absorber;
5. Back contact.

A transparent conducting oxide (TCO) is used as an antireflection coating. It can provide a low resistance contact to CdS layer. SnO_2 is traditional TCO. SnO_2 has two thin film layers. The first thin film is the fluorine doped tin oxide layer (SnO_2:F). This layer also called conductive tin oxide or c-SnO_2. It is the transparent contact that provides current collection from the front of the device. The second thin film is the undoped SnO_2 layer (also called i-SnO2 for 'intrinsic' or `insulating' SnO_2). It can help protect the open-circuit voltage of the device in some situations (Rose et al., 1999). Cd_2SnO_4 (Cadmium tin oxide, CTO) is the new development TCO. CTO has much more advantages than SnO_2, such as high conductivity and better optical property. The n-type CdS layer serves as the window layer and the CdTe layer serves as the absorber layer for the incident light. P-type CdTe films will lead to large internal resistance losses. So, in this structure, the CdTe layer is intrinsic (that is, neither p-type nor n-type, but natural), and add a layer of p-type zinc telluride (ZnTe) between the CdTe and the back electrical contact. This is n-i-p structure. The electrical field is formed between the n-type CdS and the p-type ZnTe which extends right through the intrinsic CdTe. The buffer layer ZnTe:Cu–doped graphite with high conductivity can improve the Ohmic conductance. The HgTe:Cu-doped graphite layer also can be used as buffer layer which produces an ohmic contact to the CdTe, then the silver layer is used to decrease the lateral resistivity of the back contact (Rose et al., 1999).

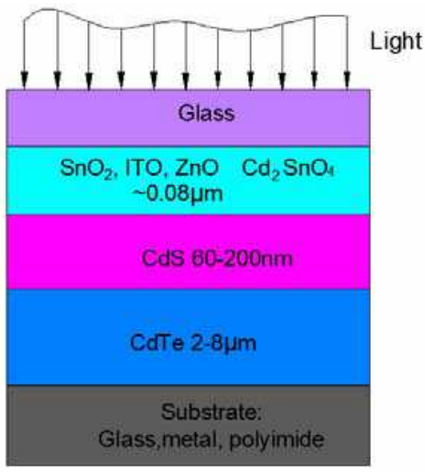

Fig. 4.2. Conventional CdS/CdTe structure

4.2.2 Unconventional structure

Base on the conventional CdS/CdTe solar cell structure, Wu. (Wu, 2004) introduced a new structure CTO/ZTO/CdS/CdTe solar cell. This structure has been developed since the year of 2001 with total-area efficiency of 16.5% (V_{oc}=845.0 mV, J_{sc}=25.88 mA/cm^2, FF=75.51%, and area=1.032 cm^2). This is the highest efficiency ever reported for CdTe solar cells.

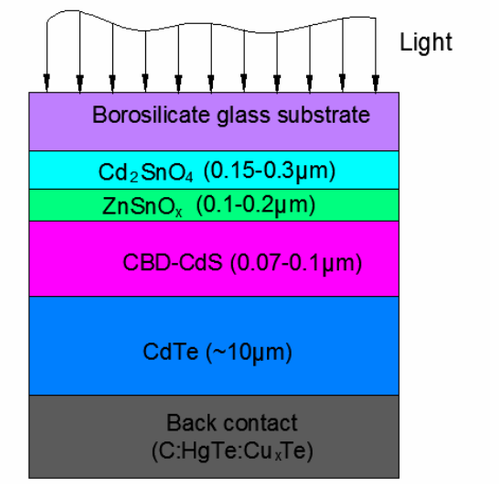

Fig. 4.3. Modified CTO/ZTO/CdS/CdTe device structure (Wu, 2004)

Figure 4.3 shows the CTO/ZTO/CdS/CdTe solar cell structure. The cadmium stannate (Cd_2SnO_4, or CTO) transparent conductive oxide (TCO) films have lower resistivity, higher transmittance and smoother surfaces than conventional SnO_2 TCO films. They can improve the Jsc and FF of a solar cell. Thin film $ZnSnO_x$ (ZTO) is a buffer layer, it can improve device performance and reproducibility. The ZTO film has a high optical bandgap (~3.6 eV) and near-zero absorbance. This device performance can be enhanced and transmission loss due to the TCO front-contact can be reduced by use of the CTO and ZTO bilayers (Wu et al., 1998; Wu et al., 2006). ZTO buffer layer can significantly reduce resistivity between the CTO and CdS layers in two reasons. First it can reduce the probability of forming a localized TCO/CdTe junction with low Voc and FF when the CdS film is thinned. Second, it can greatly reduce shunting problems (Wu et al., 2001). A buffer layer could help relieve stresses between these layers, thereby improving adhesion during the CdCl2 treatment.

Zinc stannate films have the properties of high bandgap, high transmittance, low absorbance, and low surface roughness. These films are chemically stable and exhibit higher resistivity. They can match well with CdS window layer. In fact ZTO buffer layer can significantly enhance the performance and reproducibility of both SnO_2-based and Cd_2SnO_4 (CTO)-based CdS/CdTe devices (Wu et al., 1998; Gayam et al., 2007).

4.2.3 Substrate

Soda-lime glass

Soda-lime glass is also called soda-lime-silica glass. It is the most common glass and widely used for windowpanes and glass containers (bottles and jars) for beverages, food, and some commodity items. Soda-lime glass is the basic substrate materials for CdS/CdTe thin film solar cell (Matsune et al., 2006). But soda-lime (SL) glass has poorer properties than borosilicate glass, such as a higher thermal expansion coefficient, higher Na and Fe content, higher absorbance, and lower softening temperature.

Borosilicate glass

Borosilicate glass is noted for its low thermal expansion and chemical resistance. Therefore it is widely used in laboratory equipment and near heat sources such as lamps. Borosilicate

glass is very good for thin film substrate. Corning glass is one kind of alkali free borosilicate glass. It was originally developed for thin film electronic circuits, which require an extremely smooth substrate with special electrical properties. Corning glass has very good surface flatness, surface smoothness and very low thermal expansion. The glass has an alkali level under 0.3%. This is very important since alkali ions are known to be detrimental to performance, reliability, and longevity of thin film devices. Corning glass 7059 (Wu et al., 2006; Compaan et al., 2004; Kumazawa et al., 1997; Britt & Ferekides, 1993) and 1737 (Matsune et al., 2006) are ideal substrate glass for CdS/CdTe thin film solar cell.

4.2.4 Front contact-transparent conducting oxide (TCO)

The most important characteristics that a transparent conductive oxides (TCO) front contact must exhibit are a low sheet resistance and a high transparency in the visible region. TCOs are important semiconductors thin films used on solar cells. Most of these films are fabricated with polycrystalline or amorphous microstructures. They are nanocomposites. The important TCOs are impurity-doped ZnO, In_2O_3 , SnO_2 and CdO as well as multi-component oxides consisting of combinations of ZnO, In_2O_3 and SnO_2, including some ternary compounds existing in their systems (Minami, 2005). The ternary compounds include Cd_2SnO_4, $CdSnO_3$, $CdIn_2O_4$, Zn_2SnO_4, $MgIn_2O_4$, $CdSb_2O_6$ and $In_4Sn_3O_{12}$, $ZnSnO_3$, $Zn_2In_2O_5$, $Zn_3In_2O_6$, In_2SnO_4. Sn doped In_2O_3 (ITO) and F doped SnO_2 TCO thin films are the preferable materials for most present applications. In solar cells, TCOs need meet some requirements such as low resistivity (below 10^{-3} Ω·cm) and good transmittance of incident light (over 80%). The industry standard in TCO is ITO, or tin-doped indium-oxide. This material has a low resistivity of ~10^{-4} Ω·cm and a transmittance of greater than 80%. But ITO is very expensive. Alternative materials such as ZnO:Al (AZO) and ZnO:Ga (GZO) can be the solution. Figure 4.4 gives the practical TCO used on thin film transparent electrodes. Cd containing TCOs are not listed here because of the toxicity of Cd.

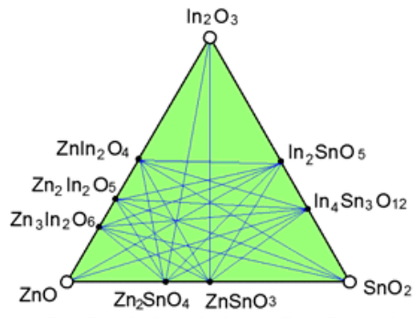

Fig. 4.4. Practical TCO semiconductors for thin-film transparent electrodes.

The study on impurity-doped ZnO, In_2O_3 and SnO_2 thin film TCO shows that the obtained minimum resistivities of impurity-doped ZnO are still decreasing and close to those of In_2O_3, whereas those of impurity-doped SnO_2 and In_2O_3 films have essentially remained unchanged for more than the past twenty years (Minami, 2005). So, AZO is the best alternative for ITO.

In the tandem thin-film solar cells, the requirements for TCO front-contact are high band-gap, high transmission and high conductivity (low resistivity). This TCO can be a transparent contact in the top cell. It must also have high transmission in the sunlight wavelength. But the conventional TCOs (such as ITO, SnO_2, and ZnO) cannot completely

meet these requirements. Wu. developed a high-quality CTO TCO film (Fig 4.3), which has transmission of 80-90% in the region 400–1300 nm and bulk resistivity of $1.8x10^{-4}\Omega \cdot cm$ (Wu, 2004). The problem of this TCO contains Cd element, it is toxic.

SnO_2:F TCO

SnO_2:F is the SnO_2 films doped with fluorine. SnO_2:F is the conventional TCO and used for more than 30 years. The SnO_2:F TCO has good absorbance (A) and transmittance (T) in the visible region (Chu et al., 1991; Wu et al., 2006; Compaan et al., 2004; Britt & Ferekides, 1993). It is a quite stable material but it exhibits a high resistance and not good for this kind of solar cells.

Indium tin oxide (ITO) TCO

Indium tin oxide (ITO) (Matsune et al., 2006; Minami, 2005) is one of the most widely used transparent conducting oxides (TCO) on thin film solar cell because of its very good electrical conductivity and optical transparency. Normally, ITO is In_2O_3, but some In can diffuse into CdS and/or CdTe when this material is used as a front contact. In this case a SnO_2 buffer layer can be used as a diffusion barrier. ITO thin film is a composite with indium (III) oxide (In_2O_3) and tin (IV) oxide (SnO_2), typically 90% In_2O_3, 10% SnO_2 by weight. It is transparent and colorless. In the infrared region of the spectrum it is a metal-like mirror. Like other transparent conducting oxides, when a compromise (In_2O_3 and SnO_2) has to be reached during its film deposition, the high concentration of charge carriers will increase the material's conductivity, but decrease its transparency. ITO thin films are most commonly deposited on surfaces by electron beam evaporation (EBE), physical vapor deposition (PVD), or a range of sputter deposition (SD) techniques.

A new TCO that is fluorine doped In_2O_3 was developed. It exhibits very good properties that the resistivity is $2x10^{-2}\Omega m$, the transparency better than 90% between 400 and 800 nm and this materials is quite stable at a temperature of 500^0C. The best CdS/CdTe solar cells with an efficiency of approximately 14% are obtained by using 0.4 μm of fluorine doped In_2O_3 as a TCO (Romeo et al., 2003).

Nano-scale ITO thin films can provide a path to a new generation of solar cells. These materials applied on solar cells can make the cells to be low-cost, ultra-lightweight, and flexible. Because of the nanoscale dimensions of the nanorods, quantum-size effects influence their optical properties. But a stable supply of indium-tin-oxide (ITO) cannot be assured because indium is a very expensive and scarce material.

The main problem about ITO is the cost. ITO's price is several times that of aluminum zinc oxide (AZO). But ITO is much better than AZO in almost every performance. For example, ITO has very good chemical resistance to moisture and it can survive in a CIGS cell for 25–30 years on a rooftop.

ZnO:Al (AZO) TCO

ITO is very expensive TCO. AZO is one of alternatives to ITO. AZO thin films, with a low resistivity of the order of $10^{-5}\ \Omega \cdot cm$ and source materials that are inexpensive and non-toxic, are the best candidates (Minami, 2005; Minami, 2008). AZO has relative good optical transmission performance in the solar spectrum. The ZnO:Al film is more transparent than SnO_2:F over the whole spectrum due to higher electron mobility. But the SnO_2:F has more better absorbance than ZnO:Al (Figure 4.5). ZnO:Al has high transparency well into the infrared and excellent sheet resistance with high mobility. Thus it is an attractive candidate

as a TCO. AZO has been used on CdS/CdTe solar cell and achieve a CdTe solar cell with 14.0% efficiency at one sun for an air-mass-1.5 global spectrum (Compaan et al., 2004).

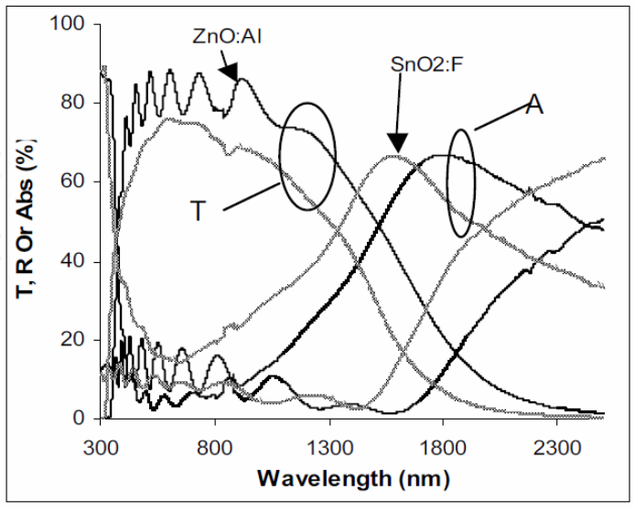

Fig. 4.5. ZnO:Al & SnO2:F optical properties (Compaan et al., 2004).
A- absorbance and T- transmittance

But In comparison to sputtered cells on commercial SnO_2:F, the stability of ZnO:Al-based cells is poorer. This may be due to interdiffusion across the ZnO:Al/CdS interface (Gupta & Compaan., 2004).

4.2.5 Back contact

The back contacts on CdS/CdTe solar cells often show a non-Ohmic behavior because of the semiconductor Schottky barrier. This Schottky barrier acts as a diode reverse biased to the CdS/CdTe junction diode and increases the contact resistance, thereby reducing the solar cell performance [Te901]. The main function of back contacts is to eliminate the Schottky barrier to reduce the contact resistance. It is well known that the addition of Cu to back-contacts is commonly used to improve the performance of CdS/CdTe solar cells. This may be due to the reaction with a Te-rich CdTe layer and the formation of a Cu_xTe/CdTe back-contact (Wu, 2006). But copper is a fast diffuser and it influences the long-term stability of such cells. Cu should be avoided in the back contact to obtain a long term stable CdTe/CdS solar cell

Conventional back contacts on CdS/CdTe solar cells are commonly made with Cu/Au or Hg (Compaan et al., 2004) or Pb and Cu/graphite (Aramoto et al., 2003). Cu-containing back contacts can influence the solar cells efficiency and the performance degrades because of Cu diffusion to the junction. Cu can easily combine with Te to form Cu_2Te. This material is unstable. In order to get stable back contacts Sb has been applied [Te901]. Sb/Au back contact also shows typical diffusion which is causing degradation just like Cu/Au back contact. But the degradation for the Sb/Au back contact is not as strong as that for the Cu/Au contact. Different back contact materials have been investigated so far, such as Cu_xTe (Wu et al, 2006), ZnTe:Cu (Wu et al, 2006), As_2Te_3:Cu (Romeo et al., 2010; Romeo et al., 2007), Bi (Vigil-Galán et al., 2007), Sb_2Te_3 (Romeo et al., 2007), even ITO (Romeo et al., 2007; Tiwari et al., 2004).

ZnTe:N/ITO (Marsillac et al., 2007) is one kind back contact of CdS/CdTe solar cell. The cell structure is SnO_2:F/CdS/CdTe/ZnTe:N/ITO. After $CdCl_2$ treatment, ZnTe:N was achieved through sputtering an undoped ZnTe in a 5% nitrogen–95% argon environment. Then ITO thin film was deposited. Because the ZnTe:N layer is too thin and the conductivity of the ZnTe:N film is not very high, a secondary transparent electrode was used to collect the photogenerated current. ITO TCO film can be used as the secondary transparent electrode. This back contact is the same as Cu_xTe/ITO (Wu et al, 2006). It is for ultra-thin absorber (eta) soalr cell. This back contact is transparent just like transparent front contact. It can be used in polycrystalline thin-film tandem cells because there is enough light transmitted to the bottom cell (Romeo et al., 2007; Tiwari et al., 2004). TCO back contact on CdTe provides superior cell stability, simplified processing and a potential for low-cost production. The average efficiency of reference solar cells with standard Cu/Au back contacts on CdTe is in the range of 10-11%. It was observed that most of the solar cells with ITO back contact were in the efficiency range of 7-8%. A. N. Tiwari et al developed a kind of CdTe solar cell with SnO_2:F as a front contact for CdS and ITO as a back contact on CdTe. The efficieny achieved 7.9% (V_{oc}=702mV, J_{sc}=18.2 mA/cm^2, FF=0.62) (Tiwari et al., 2004).

4.2.7 Fabrication

Fabricating CdTe solar cell includes a serial deposition processes such as TCO layer, CdS layer, CdTe layer, and back contact layer etc deposition processes. Each individual process has many deposition methods such as CBD, CSS, CVD, Ed and sputtering process etc. Figure 4.6 gives the deposition processes of one example of conventional structure and one

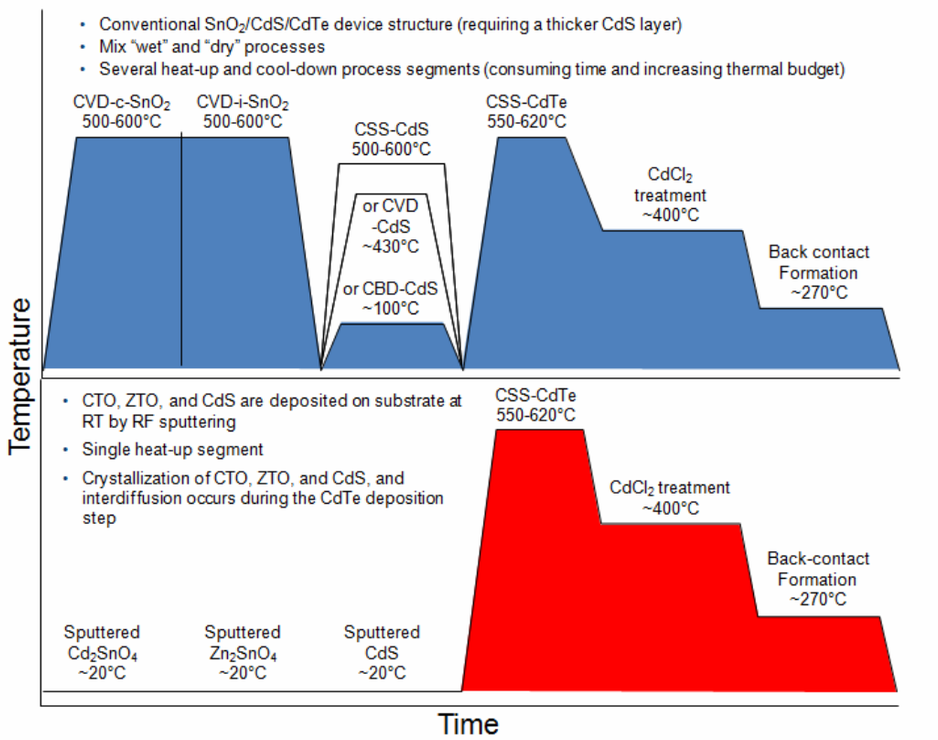

Fig. 4.6. The conventional solar cell and CTO/ZTO/CdS/CdTe solar cell deposition process (Noufi, 2006).

example of CTO/ZTO/CdS/CdTe device structure (Noufi, 2006). For conventional structure, both SnO_2 (c-Sno_2 and i-SnO_2) can be deposited on glass by CVD; thin film CdS is formed on SnO_2 layer by CBD, CVD or CSS; CdTe film is deposited by CSS. CSS has received the most attention for CdTe deposition recently because it is well-suited to large-scale manufacturing (Rose et al., 1999).

For the CTO/ZTO/CdS/CdTe structure, the first three layers Cd_2SnO_4 (CTO), Zn_2SnO_4 (ZTO) buffer layer and CdS window layer are prepared by the same deposition technique-RF magnetron sputtering at room temperature. RF sputtering is a mature technology with many advantages such as thickness control and easy operation. This deposition process has only one heat-up segment (CdTe CSS process) in the entire device fabrication process. In the CdTe CSS process, the recrystallization of the first three layers and the elements interdiffusion at the three interfaces (CTO/ZTO, ZTO/CdS and CdS/CdTe interfaces) are completed. This kind of solar cell can reach efficiency of 14.7% (Voc = 833.8 mV, Jsc = 24.06 mA/cm2, FF = 73.29%, and area=1.159cm^2) (Wu, 2004).

After CdTe CSS deposition, there is a $CdCl_2$ annealing in both processes. The main effect of the $CdCl_2$ heat treatment on the physical properties of CdTe thin films is to promote recrystallization and grain growth. But here the CSS process is in a higher temperature and has large grain size. The recrystallization process has finished in CdTe CSS process. $CdCl_2$ treatment has several substantial benefits such as: grain-boundary passivation, increased CdS/CdTe interface alloying, and reduced lattice mismatch between the CdS and CdTe layers. The ZTO ($ZnSnO_x$) films were deposited by RF sputtering at room temperature which has a very high resistivity. After $CdCl_2$ annealing at a higher temperature, the film resistivity is reduced greatly. The ZTO band-gap (Eg) remains the same (~3.6 eV), but its optical transmission is slightly improved. The reason is the inter-diffusion at the interfaces. The inter-diffusion of the CdS and ZTO layers improved the quantum efficiency of a CdTe cell over the entire active wavelength region (400-860 nm). Even in the conventional device structure, the inter-diffusion also can improve device performance and reproducibility. In spite of the 9.7% lattice mismatch between hexagonal CdS and cubic CdTe, this structure still can get very high efficiency due to the interdiffusion. After anneal, the V_{oc} and FF increase, so does the efficiency. Cells made without the anneal generally have efficiencies between 6% and 10%, whereas cells made with the anneal are generally more than 12% efficient. (Wu et al., 2005; Rose et al., 1999; Wu et al., 2004).

4.2.8 Cu in CdS/CdTe solar cell

K. Barri et al has studied the role of copper in CdTe solar cell. Copper is typically introduced in CdTe during the application of the back electrode, to enhance device performance by facilitating the formation of an ohmic back contact. But Cu and Te can form unstable component Cu_2Te, which is associated with long time stability (Barri et al, 2005, Dobson et al., 2000). Here, Cu was introduced in the CdS film prior to the deposition of the CdTe and both plain graphite and Sb_2Te_3/Mo were used as back contacts (Fig.4.7). The high performance of the solar cell achieved (V_{OC} of 830 mV and FF's in the high 60's) clearly indicates that Cu enhances device performance, even when intentionally introduced in CdS. But excessive amounts of Cu can lead to shunting and poor collection. The formation of Cu_2Te may not be necessary to achieve effective back contacts to CdTe (Barri et al, 2005).

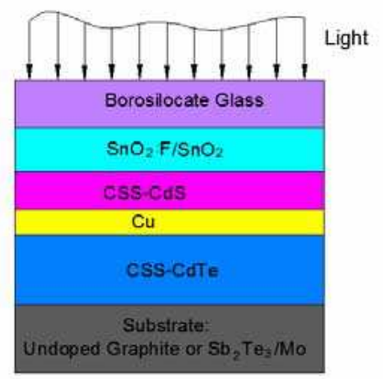

Fig. 4.7. Cu was incorporated into the device prior to the CdTe deposition (Barri et al, 2005)

4.2.9 Thickness influence

Large scale manufacturing of CdS/CdTe solar cells is constrained by the cadmium and tellurium materials. Because the tellurium is rare element and limited availability and the cadmium is hazardous to human health. Gupta et al (Gupta et al., 2006) found that it is possible to reduce the CdTe layer thickness without much compromise in efficiency. Normally the thickness of CdTe is about 2-8μm. But in the ultra-thin films solar cells, the thickness is 0.7-1.28μm. The CdS/CdTe solar cells were fabricated using magnetron sputtering method. The best thin CdTe cell was obtained with 1μm CdTe and had efficiency of 11.9%. Cells with 0.7 μm CdTe show efficiency 11.2%, this is the thinnest CdTe cell ever reported with efficiency above 10%. The standard CdTe cells (2.3 μm CdTe thickness) efficiency is 13%.

The thickness of CdS film is a critical factor affecting cell performance. Kumazawa et al (Kumazawa et al., 1997) made this study. As the thickness of CdS film decreases, the open-circuit voltage (V_{oc}) becomes low and when the CdS film thickness is less than 60nm the V_{oc} decreases dramatically. The short-circuit photocurrent density (J_{sc}) becomes a little higher when the thickness of CdS decreases (figure 4.8). It shows that CdS thickness best range is ~60 nm.

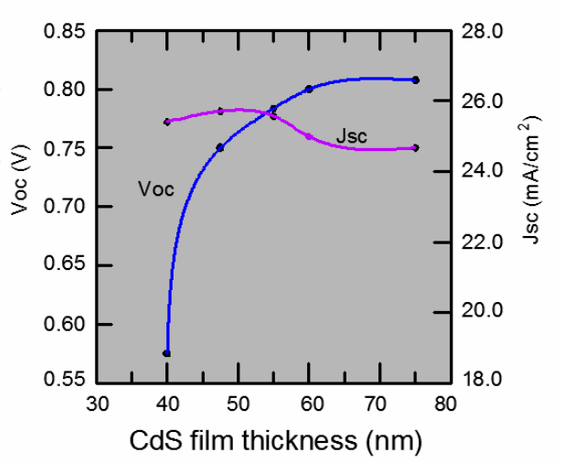

Fig. 4.8. The V_{oc} and J_{sc} as a function of CdS film thickness
Data comes from (Kumazawa et al., 1997)

4.2.10 Other type CdTe structure

1. ZnO/CdTe/CuSCN heterostructure (Tena-Zaera et al., 2005)

This structure can be made as eta (extremely thin absorber) solar cell. It uses SnO_2:F as the TCO. ZnO/CdTe is an n-type window layer semiconductor and CuSCN is a p-type absorber layer semiconductor. The energy gap of ZnO is 3.31 eV and that of CdTe is 1.54 eV. In the 400–800 nm (AM1.5) solar spectrum range, the effective absorption (AE) is about 87% and the effective reflectance (RE) is only 10%. It is very favorable for the use of extremely thin absorber (eta) solar cell. TiO_2/CdTe/ZnTe and TiO_2/$CuInS_2$/CuSCN have the similar heterostructures as that of ZnO/CdTe/CuSCN.

2. Au–Cu/p–CdTe/n–CdO/glass-type solar cells (Santos-Cruz et al., 2006)

The CdO:F films were grown by the sol-gel method, The resistivity is $4.5X10^{-4}\Omega$·cm and the optical transmission is higher than 85%. The CdTe:Sb films were prepared by the RF sputtering technique, the resistivity value is $10^6\Omega$·cm.The Au–Cu contacts were thermally evaporated. This kind of heterostructure PV solar cell can achieve the highest energy conversion efficiency 5.48%.

3. ZnS and ZnCd as window layer (Contreras-Puente et al., 2000)

G. Contreras-Puente et al developed SnO_2/$Zn_{0.9}Cd_{0.1}$/CdTe and SnO_2/ZnS/CdTe two types semiconductor thin films solar cells. The efficiencies are 1.26% (V_{oc} = 489 mV, J_{sc} = 8.9 mA/cm^2, FF = 29%) and 3.12%((V_{oc} = 324 mV, J_{sc} = 22 mA/cm^2, FF = 42%) respectively. The efficiencies are very low.

4.2.11 CdTe/CdS Solar cells on flexible substrates

Normally, the substrates of thin film CdS/CdTe solar cells are glass. But glass are hard, weight and fragile. The post deposition annealing of the films needs a high temperature (420˚C). This temperature can cause rupture of the glass substrate. On the other hand, solar cells on flexible metallic substrates are light weight, free of damage and are suitable for storage, transportation and installation. CdTe has been successfully electrodeposited on various foils such as stainless steel (SS), Mo, Ni and Cu. Molybdenum is considered as the suitable substrate material from the point of view of the matching thermal expansion coefficient with CdTe. Pantoja Enriquez et al (Pantoja Enriquez et al., 2004) developed a CdTe/CdS device on flexible molybdenum (Mo) substrate with the efficiency of 3.5% (Voc=0.5 V, Jsc=10.6mAcm^{-2}, FF=0.4).

Figure 4.9 gives another unconventional CdS/CdTe solar cell structure (Singh et al., 1999)

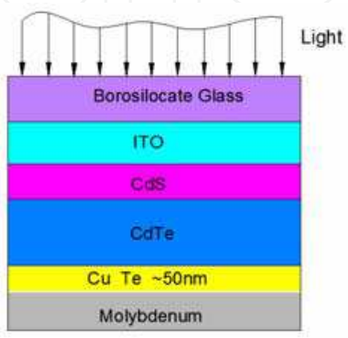

Fig. 4.9. Schematic of device configuration on Mo foil substrate (Singh et al., 1999)

The substrate is molybdenum foil. CdS is deposited on top of CdTe. Thin film inter-layers (approximately 50 nm thick) of Cu and Te are used to improve the conductivity between Mo and CdTe. Thin film Cu and Te has the same role of ZnTe as in fig. 4.1. Cu and Te can dope CdTe and make it heavily p-type, which facilitates tunneling. Also Cu and Te can form compound $Cu_{2-x}Te$ between Mo and CdTe and make tunneling more effective. This structure is made as follows: Inter-layers of Cu and Te are evaporated onto the Mo substrate; CdTe is deposited by thermal evaporation and then treated with a $CdCl_2$ solution and annealed; CdS film is deposited by thermal evaporation and then treated with $CdCl_2$, annealed and indium doped. The thermal evaporation processes are in low temperature (220˚C), so $CdCl_2$ treatment has two functions: one is to promote the diffusion of Te and Cu into CdTe to create a p-type region and improve the conductivity between CdTe film and molybdenum; the other is to promote crystal growth of CdTe and CdS through recrystalization. The top contacting material is made by sputtering ZnO, ITO or a combination of ZnO and ITO. This molybdenum foil substrate solar cell cannot get such high efficiency as that of glass substrate solar cell. One reason is the high series resistance of the device, The other reason is that the high defect density associated with rough CdTe/CdS interface, which results in low shunt resistance.

Matulionis et al (Matulionis et al., 2001) made the same structure of Mo/CdTe/CdS/ITO thin-film solar cells by radio-frequency magnetron sputtering. The conversion efficiency is 7.8 percent on 0.05 cm^2 area device. The high efficiency is due to the back contact. Here, the back contact between the molybdenum and the CdTe is ZnTe:N, it can improve the conductivity.

Au/Pd alloy layer also can be the interlayer between Mo substrate and CdTe layer (Pantoja Enriquez et al., 2004).

The polymer also can be the substrate of CdTe/CdS solar cell. The problems of this substrate are low light absorption and high temperature stability. The highest reported efficiency of a flexible CdTe/CdS solar cell on polymer substrate is 11.3% (Romeo et al., 2006). This efficiency can compare well with the efficiency of CIGS or a-Si solar cells developed on polymer foils.

4.3 Cu(In, Ga)Se_2 (CIGS) thin film solar cell

Copper indium gallium (di)selenide (CIGS), is a compound semiconductor material composed of copper, indium, gallium, and selenium. It is used as light absorber material for thin-film solar cells. The chemical formula of this material is $CuIn_{(1-\chi)}Ga_{\chi}Se_2$, where the value of χ can vary from 0 to 1. When χ is 0, it is copper indium selenide (CIS) and when χ is 1, it is copper gallium selenide (CGS). In laboratory research, the efficiency of CIGS solar cell is approaching 20%. CIGS solar cell can be deposited on a variety of cheap substrates (e.g., glass, plastic, foil) and has acceptable environmental stability characteristics. There is no toxic Cd in the absorber layer, even the window layer (CdS) can be replaced by Cd-free materials. These advantages attract much focus on CIGS-based devices.

Depending on the Ga/(In+Ga) ratio, the bandgap of CIGS can be varied continuously between 1.04 (CuInSe2) and 1.68 eV (CuGaSe2). The current high-efficiency devices are prepared with bandgaps in the range 1.20–1.25eV, this corresponds to a Ga/(In+Ga) ratio between 25 and 30% (Romeo et al., 2004).

Compared with CdTe thin film solar cell, CIGS solar cell absorber layer is complex. It has four elements as Cu, In, Ga and Se. The properties of the device are significantly impacted

by the detailed compositional profile in the absorber. CuInGaSe2 has some drawbacks due to limited availability and increasing cost of indium and gallium elements.

CIS, CIGS,CGS and Ga grading

CIS is an abbreviation of copper indium selenide ($CuInSe_2$). If added gallium, it will become CIGS. CGS is an abbreviation of copper gallium selenide (CuGaSe2). If added indium, it change to CIGS. So, CIGS is a variation of CIS or CGS. CuInSe2 and CuGaSe2 have the chalcopyrite lattice structure; it is a diamond-like structure. CIS and CGS have high optical absorption coefficients and versatile optical and electrical characteristics and is especially attractive for thin film solar cell application. CIS (no Ga) and CGS (no In) solar cells have achieved 15% and 10.2% efficiencies respectively (NERL) (AbuShama et al., 2004). At present the manufacture of CIS or CGS solar cells is high when compared with amorphous silicon solar cells. The use of gallium increases the optical band-gap of the CIGS layer as compared to pure CIS, thus increasing the open-circuit voltage, but decreasing the short circuit current. Figure 4.10 gives the CIS Ternary phase diagram.

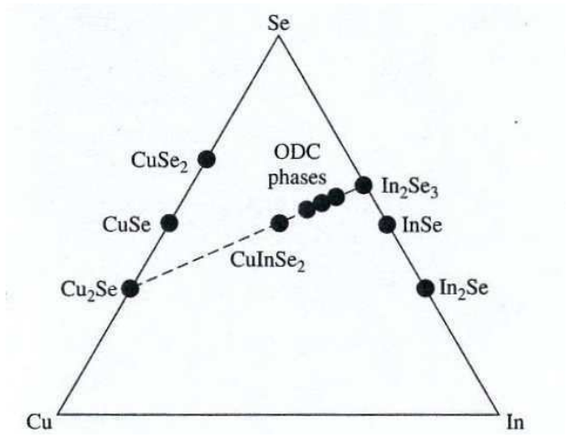

Fig. 4.10. Ternary phase diagram of the Cu-In-Se system (Anderson et al., 2003)

The binary phase Cu_2Se and In_2Se_3 can be alloyed to form $CuInSe_2$; similarly the binary phase Cu_2Se and Ga_2Se_3 can be alloyed to form $CuGaSe_2$. Ternary phase $CuInSe_2$ can be alloyed in any proportion (χ) with ternary $CuGaSe_2$ to form $Cu(In,Ga)Se_2$. The chemical formulas as follows:

$Cu_2Se+In_2Se_3 \rightarrow 2CuInSe_2$

$Cu_2Se+Ga_2Se_3 \rightarrow 2CuGaSe_2$

$(1-\chi)CuInSe_2+\chi CuGaSe_2 \rightarrow CuIn_{\chi}Ga_{1-\chi}Se_2$

So, $Cu(In,Ga)Se_2$ can accomodate large variations in composition. The compositional ratios of Cu/(In+Ga) and Ga/(In+Ga) play critical roles on the characteristics of CIGS solar cells. The Cu/(In+Ga) ratio largely affects the morphology of the CIGS absorber, while the Ga/(In+Ga) ratio determines the band-gap, both of which are critical for cell performance (Sakurai et al., 2003).

The ratio (χ) of Ga/(In+Ga) can change the band-gap of the CIGS absorber layer. According to different Ga/(In+Ga) ratio, the CIGS solar cells with different band-gap can be manufactured. The most important is this ratio not only to optimize the general band gap level, but also to obtain different band gaps at different depths in the CIGS thin film. This is

called band gap profiling. In CIGS thin film solar cells an in-depth band gap variation due to changes in the Ga/(In+Ga) ratio is commonly referred to as Ga-grading (Lundberg et al., 2005). By increasing the Ga/(Ga+In) ratio (χ) from 0 to 1 the band-gap varies continuously from about 1.02 eV (CIS) to about 1.66 eV (CGS). The various band gaps are suitable to the solar spectrum to improve light absorption and thereby further improve the solar cell performance and increase the efficiency. For high performance devices, the ratios are Ga/(In+Ga)=0.2-0.3 and Cu/(In+Ga)=0.7-1.0. In the recorded high efficiency (19.9%) CIGS solar cell, the ratios are Ga/(In+Ga)=0.3 and Cu/(In+Ga)= 0.81 (Repins et al., 2008).

4.3.1 Structure of a CIGS thin-film solar cell

CIGS thin film solar cell has the same structure as CdTe solar cell (Figure 4.2). It has 5 different thin film layers as:

1. Substrate;
2. Front contact-Transparent conducting oxide (TCO);
3. CdS window layer;
4. CIGS absorber;
5. Back contact.

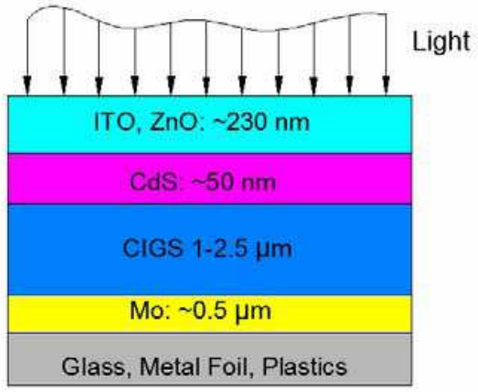

Fig. 4.11. CIGS thin-film solar cell structure.

Basic CIGS thin film solar cell structure is depicted in Figure 4.11. The Individual layer thicknesses are approximate and may differ somewhat among laboratories. The substrates can be glass (NAKADA & MIZUTANI, 2002), metal foils (Wuerz et al., 2009) or plastics (Huang et al., 2004). The most common substrate is soda-lime glass, which is about 1–3 mm thickness. Metal molybdenum (Mo) is coated on the substrate as back contact pole (NAKADA & MIZUTANI, 2002). The semiconductors CIGS, CdS and ZnO are shaped into the heterojunction. Here CIGS is p-type semiconductor and ZnO is n-type semiconductor. CdS is buffer layer. In this asymmetric structure, the CIGS layer serves as an absorber, ZnO and CdS layers serve as window layers and the band-gaps: $E_{g,ZnO}$=3.2 eV and $E_{g,CdS}$=2.4 eV. ZnO layer also serves as front contact pole for current collection.

CIGS absorber layer is complex, according to detailed thin film composition. It can be CIS, CIGS or CGS.

CdS window layer can be replaced by ZnS etc thin film to realize Cd-free thin films CIGS solar cells. Front contact TCOs can be ZnO (Repins et al., 2008), ZnO:Al (NAKADA & MIZUTANI, 2002), ITO etc. Back contact can be Mo (formation of $MoSe_2$, back surface field), Cr (Na barrier), Cu (CIS Cut process) or TCOs (superstrate cells, reversed configuration).

The standard thickness of the Cu(In,Ga)Se_2 (CIGS) absorber thin film layer is 1–2.5 μm (Figure 4.11). Reducing the thickness can reduce the materials cost and lower the production cost. Lundberg et al (Lundberg et al., 2003) research shows that when the thickness of the CIGS absorber layer is down to 0.8-1.0 μm, this structure can maintain a very high performance. When the CIGS layer was further reduced in thickness the loss in performance increased. When the thickness is 1.8 μm, the efficiency is 16.1%; when the thickness is 1.0μm, the efficiency is 15%; but when the thickness is 0.6 μm, the efficiency is 12.1%. A pronounced loss in the efficiency is shown.

4.3.2 Manufacturing

The CIGS layer can be deposited in a polycrystalline form directly onto molybdenum coated glass sheets or steel bands. Compared to large crystal, it can save energy. CIGS films can be manufactured by several different methods. A vacuum-based process (NAKADA & MIZUTANI, 2002; Repins et al., 2008; Delahey et al., 2004) is very common. Co-evaporating or co-sputtering copper, gallium, and indium can form a CuInGa thin film. Then the film is annealed in a selenide vapor to form the CIGS structure. The CIGS also can be formed with directly co-evaporating copper, gallium, indium and selenium onto a heated substrate. A non-vacuum-based process deposits nanoparticles of the precursor materials on the substrate and then sinters them in situ. CIGS layer also can be achieved through electroplating, which is the low cost way. Vacuum processes are expensive and can achieve very high efficiency of almost 20% (NAKADA & MIZUTANI, 2002; Repins et al., 2008). Non-vacuum solution processes progressed quickly and can get efficiencies of 10%-15% (Bhattacharya et al., 2001; Kapur et al., 2003), such companies as ISET, Nanosolar and IBM have this technology.

The recorded high efficiency (19.9%) CIGS solar cell deposition process is so-called three-stage process introduced by NREL (Gabor et al., 1994). It is a vacuum process. In first stage, In, Ga and Se are co-deposited to form $(In_x,Ga_{1-x})_2Se_3$, followed by the co-deposition of Cu and Se until Cu-rich composition CIGS is reached, and finally the overall Cu concentration is readjusted by subsequent deposition of In, Ga and Se. The process yields smooth films and can result in compositional profiles contributing to both high currents and voltages in the devices. This smoother surface facilitates the uniform conformal deposition of a thin buffer layer and prevents ion damage in CIGS during sputter deposition of ZnO/ZnO:Al (Gabor et al., 1994; Pomeo et al., 2004). The overall solar cell is made as follows: Soda-lime glass (SLG) substrate, sputtered Mo back contact, three stage co-evaporated CIGS, chemical-bath-deposited (CBD) CdS, sputtered resistive/conductive ZnO bi-layer, e-beam-evaporated Ni/Al grids, MgF2 antireflective coating, and photolithographic device isolation (Repins et al., 2008; Contreras et al., 1999; Ramanathan et al.,2003).

There are many deposition processes of CIGS thin film. Co-evaporation and two-step are the main processes (Shafarman & Stolt., 2003). Figure 4.12 shows the schematic of co-evaporation process.

The process uses line-of-sight delivery of the Cu, In, Ga, and Se from open-boat sources to the heated substrate. The source evaporation temperature is under control. Typical ranges are 1300 to 1400°C for Cu, 1000 to 1100°C for In, 1150 to 1250°C for Ga, and 300 to 350°C for Se evaporation. The advantage of the coevaporation process to deposit CIGS thin film is its considerable flexibility to choose the process specifics and to control film composition and band gap. The disadvantage is the difficulty in control, particularly the control of the Cu-evaporation source. The deposition, diagnostic, and control technology need be improved.

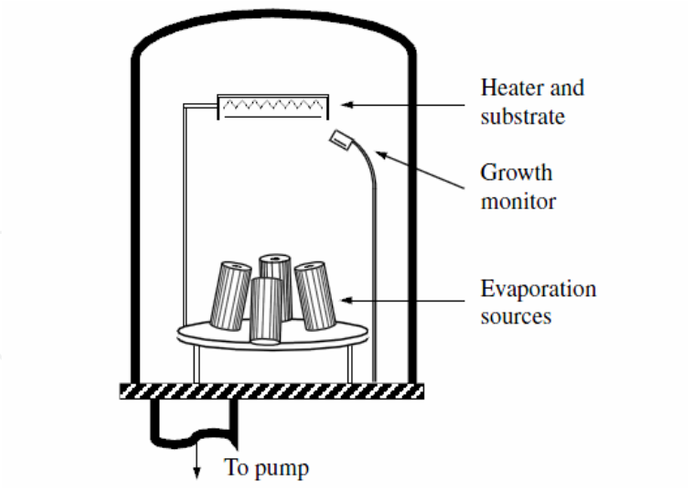

Fig. 4.12. Configuration for multisource elemental coevaporation.
(Shafarman & Stolt., 2003).

Two-step process is also called selenization. In selenization, copper, indium and gallium source atoms are ejected from solid targets by high-energy ions (also called "sputtering"). The selenium is added in a second step through a "selenization" process using a high temperature hydrogen selenide gas or solid source selenization. Sputtering is a mature technique. This is the primary advantage of selenization. But this process has the limited ability to control composition and increase band gap, which may limit device and module performance. Other difficulties that must be overcome include poor adhesion and the use of hydrogen selenide, which is hazardous and costly to handle.

Other Deposition includes hybrid sputtering in which Cu, In, and Ga are sputtered while Se is evaporated, closed space sublimation (CSS), chemical bath deposition (CBD) etc. These methods are reviewed in Reference (Shafarman & Stolt., 2003).

CIGS thin film solar cells have become commercial products successfully. A lower-cost process should feature high deposition rates, high material utilization, and simpler equipment capable of processing very large substrates. In order to lower the cost, there are still some critical issues for CIGS application (Ullal, H.S. & Roedern, B. von. 2007):

1. Standardization of equipment and technology for the growth of the CIGS absorber films;
2. Higher module efficiencies (over 20%);
3. Prevention of moisture ingress for flexible CIGS modules;
4. Thinner absorber layers of less than 1 micrometer or less;
5. CIGS absorber film stoichiometry and uniformity over large areas.

4.3.3 Efficiency

CIGS ($CuIn_xGa_{(1-x)}Se_2$) is one of the most prospective absorber materials for low cost polycrystalline thin film solar cells. Unlike the homojunction silicon cells, the structure of CIGS cells is a more complex heterojunction system. CIGS solar cell can achieve very high efficiencies such as 19.5% (x~0.3) (Contreras et al., 2005) ,19.9% (x~0.3) (Repins et al., 2008) etc. In National Renewable Energy Laboratory (NREL), the new world record total area efficiencies of 15.0% for CIS and 10.2% for surface modified CGS solar cells had been

achieved. The use of gallium increases the optical band gap of the CIGS layer as compared to pure CIS, thus increasing the open-circuit voltage. Crystalline silicon solar cells can get efficiency as high as 24.7%, and CIGS efficiency is lower than 20%. But CIGS is much cheaper due to the much lower material cost and potentially lower fabrication cost. CIGS has very strong light absorption as a direct band-gap material. Most of the sunlight can be absorbed with 1-2um thickness CIGS layer. Compared to CdTe solar cells, CIGS are more pro-environmental solar cells. Because CIGS can consume smaller cadmium than CdTe, and cadmium is toxic material. Table 4.2 lists some conventional CIGS solar cell efficiencies.

CIGS cell	Efficiency (%)	Voc (mv)	Jsc (mA/cm2)	FF (%)	Area (cm2)	Reference
Thin-film ZnO/CdS/CIGS	19.9	690	35.5	81.2	0.419	Repins et al., 2008
Thin-film ZnO/CdS/CIGS	19.5	690	35.22	79.9	0.409	Contreras et al., 2005
Thin-film ZnO/CdS/CGS	10.2	823	18.61	66.77	0.419	AbuShama et al., 2005
Thin-film ZnO/CdS/CIS	15	490	40.5	75.2	0.403	AbuShama et al., 2005
Thin-film ZnO/CIGS	18.5	670	35.11	78.8	0.402	Kazmerski, 2004

Table 4.2. CIGS solar cell efficiencies

4.3.4 Cd-Free Cu(In, Ga)Se2 thin-film solar cells

The recent trend in buffer layers is to substitute CdS with 'Cd-free' wide-bandgap semiconductors and to replace the CBD technique with in-line-compatible processes. The standard device structure of $Cu(In,Ga)Se_2$ (CIGS)-based solar cells use a very thin chemical-bath-deposited (CBD) CdS buffer layer as window layer. But Cd is a kind of toxic materials. In the last decade, serious efforts to substitute the CdS buffer layer by other nontoxic low-absorbing materials have been made and the results are encouraging. For example, M.A. Contreras et al (Contreras et al., 2003) developed a Cd-free $Cu(In,Ga)Se_2$ thin-film solar cell. Thin film ZnS is used as window layer, which is a wider band gap material than CdS and can improve the quantum efficiency at short wavelengths. This structure solar cell can get energy conversion efficiency as high as 18.6%. This result suggests that CIGS thin film solar cells with efficiencies as high as those fabricated using CdS buffer can be achieved even if toxic Cd compounds are not utilized.

As an alternative to CdS, various materials show promising results. CBD-ZnS, MOCVD-ZnSe, ALD-ZnSe, CBD-ZnSe, CBD-ZnO, co-sputtered (Zn,Mg)O, CBD-$In(OH)_3$, ALCVD-In_2S_3, Co-evap-In_2Se_3, Co-evap-$InZnSe_x$, CBD-SnO_2 etc can be alternative buffer layers to replace the traditional CdS window layer and realize the Cd-free CIGS solar cells. The deposition methods can be: chemical bath deposition (CBD), atomic layer chemical vapour deposition (ALCVD), metal organic chemical vapour deposition (MOCVD), ion layer gas reaction (ILGAR), sputtering, thermal evaporation, and electrodeposition (ED) (Hariskos et al., 2005). Some processes can get very high efficiencies. CBD ZnS based buffer layer CIGS solar cells have 18.6% efficiency which is comparable with the CBD CdS. However, Zn-based compounds tend to form a blocking barrier due to the band alignment with CIGS. If the layer thickness is less than 50 nm, and the deposition quality is high, and the CIGS surface is uniform, the barrier can be reduced (Remeo et al., 2004). Hariskos et al has over-viewed the development of Cd-free materials and manufacture for $Cu(In,Ga)Se_2$-based thin-

film solar cells and modules. Table 4.3 lists some CIGS solar cells condition with different buffer layer materials.

Material	Method	Efficiency (%)	Reference
CdS	CBD	19.9	Repins et al., 2008
ZnS-based	CBD	18.6	Hariskos et al., 2005
$In(OH)_3$:Zn-based	CBD	14	Tokita et al., 2003
In_2S_3-based	ALCVD	16.4	Naghavi et al., 2003
ZnSe-based	CBD	15.7	Ennaoui et al., 2001
ZnInSex	Coevap.	15.3	Hariskos et al., 2005
InxSey	Coevap.	13	Hariskos et al., 2005
ZnMgO	Sputtering	16.2	Negami et al., 2002
ZnO	CBD	15.7	Hubert et al., 2009
SnO_2	CBD	12.2	Hariskos et al., 2005

Table 4.3. CIGS efficiencies and manufacture with different window layers (Hariskos et al., 2005).

4.4 Nanocomposite application in dye-sensitized solar cells

A dye-sensitized solar cell (DSSC or DSC) is a low-cost solar cell like CdTe and CIGS thin film solar cells. DSSC has developed many years, but for a very long time the energy conversion efficiency is less than 1%. The high efficiency DSSC solar cell (over 7%) was invented by Michael Grätzel and Brian O'Regan at the École Polytechnique Fédérale de Lausanne (one of the two Swiss Federal Institutes of Technology) in 1991 (O'Regan & Grätzel., 1991). For this significant discovery, DSSC solar cell attracted considerable attention as a potential alternative to conventional inorganic photovoltaics and developed rapidly during the 1990s. Dr. Grätzel created DSSC solar cell from low to medium-purity materials through low-cost process, which exhibits a commercially realistic energy-conversion efficiency. So, DSSC solar cell is called as Grätzel cell also. Up to date, the DSSC solar cell can reach 11.1% efficiency (CHIBA et al., 2006; Han et al., 2006).

DSSC can be classified into the group of nanocomposite thin film solar cells. It is based on a semiconductor formed between a photo-sensitized anode and an electrolyte, a photoelectrochemical material. Because of the high surface area of the semiconductor film and the ideal spectral characteristics of the dye, the device harvests a high proportion of the incident solar energy flux (46%) and shows exceptionally high efficiencies for the conversion of incident photons to electrical current (more than 80%) (O'Regan & Grätzel., 1991). DSSC solar cell is insensitive to temperature change. When the temperature rises from 20 to 60°C, which is the normal natural condition, the power conversion efficiency has no change. In contrast, conventional silicon cells exhibit a significant decline over the same temperature range amounting to about 20%. DSSC solar cell has the lower sensitivity to angle of light incidence as compared to silicon-based cells. These advantages made DSSCs attractive for practical applications (Grätzel, 2004). Unlike solid semiconductor solar cell, the dye-sensitized solar cell uses liquid electrolyte to transport electron excited by sunlight. The liquid electrolyte dye-sensitized solar cell has some problems such as leaking and

degradation. It is not stable. So colloids are developed and used in dye-sensitized solar cells. Normally a dye-sensitized solar cell uses nano-crystalline TiO_2 as the semiconductor material (O'Regan & Grätzel., 1991). Here the semiconductor is solely used for separating charge. Photoelectrons are generated from the photosensitive dye. Photovoltaic performance of the solar cell depends remarkably on the semiconductor materials.

4.4.1 DSSC solar cell structure and working cycle

Figure 4.13 is a schematic diagram of a DSSC solar cell. A typical DSSC includes back contact transparent conducting oxide (TCO), semiconductor titanium dioxide (TiO_2) thin film, electrolyte (usually a ruthenium bipyridyl complex), Pt catalyst and front contact TCO. The two transparent conducting oxide (TCO) glass slides are coated with fluorine doped tin oxide (FTO). TCO can be ZnO, ITO and SnO_2 etc. TCO in DSSC solar cell has the same functions with that in CdTe and CIGS solar cells. The n-type semiconductor TiO_2 thin film is attached to the substrate serves as a back electrode. The electrolyte contains a reduction-oxidation (redox) couple (I^- / I_3^-). The counter electrode TCO glass is covered with a very small amount of platinum (5–10 μg/cm²), which is responsible for catalytic cathodic reduction of triiodide to iodide. The electrolyte fully fills the space between the two electrodes.

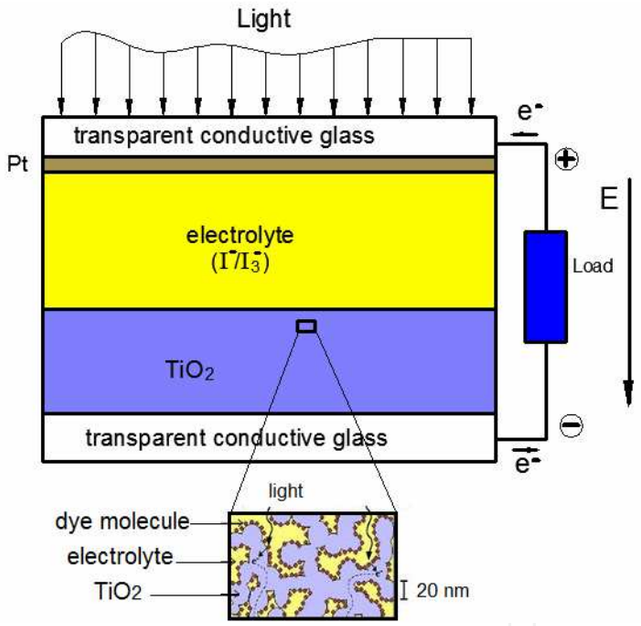

Fig. 4.13. A schematic diagram of structure and components of a DSSC solar cell
http://www.umk.fi/en/newsletter_newsletter_0108_Aitola_more.html

The semiconductor TiO_2 thin film is about 10μm thickness with the particles in nano-size about 20nm (O'Regan & Grätzel., 1991). Dye molecules are attached to the TiO_2 surface. TiO_2 is porous nano-crystalline structure and the internal surface area is thousands of times greater than the dimension of the cell (Yongbai, 2007). Under solar radiation, the dye molecules absorb the photons and excite electrons. The charge separation from the dye to the TiO_2 happens at the surface between the semiconductor and electrolyte surface. The application of porous nanocrystalline TiO_2 semiconductor and organic electrolytes

(ruthenium complex) was Dr. Grätzel's great invention. The smooth surface between electrolyte and non-porous crystalline TiO_2 can absorbs incident light less than 1%. But the interface between electrolyte and porous nanocrystalline TiO_2 can absorb incident light over 80%.

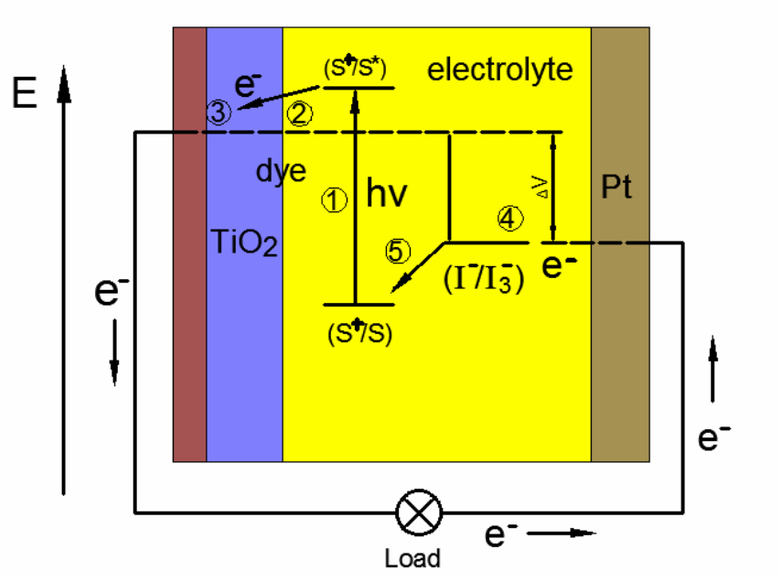

Fig. 4.14. Principle of operation and energy level scheme of the dye-sensitized nanocrystalline solar cell. Potential are referred to the standard calomel electrode (SCE) (Hagfeldtt & Grätzel, 1995). The redox system is iodide/triiodide-based redox eletrolyte. S stands for sensitizer; S*, electronically excited sensitizer; S^+, oxidized sensitizer

The DSSC is different with any other solar cells. This photovoltaic device uses molecules to absorb photons and convert them to electric charges without the need of intermolecular transport of electronic excitation, whereas others use atoms. DSSC solar cell separates the two functions of light harvesting and charge-carrier transport, whereas conventional and all of the other known photovoltaic devices perform both operations simultaneously (Grätzel, 2009). Figure 4.14 shows the DSSC solar cell working cycle and the relative energy levels of the cell. Incident sunlight passes through the transparent electrode into the dye layer where it can excite electrons that then flow into the semiconductor TiO_2 layer. The electrons flow toward the transparent electrode where they are collected for powering a load. After flowing through the external circuit, they are re-introduced into the cell on a metal electrode on the back, flowing into the electrolyte. The electrolyte then transports the electrons back to the dye molecules. This cycle includes 5 steps of photoelectronic chemistry process (Figure 4.14) (Yongbai, 2007):

1. An incident photon is absorbed by the dye molecule and an electron from a molecular ground state S is then excited to a higher energy state S* (at anode);

$$S + h\nu \rightarrow S^+ \quad (1)$$

2. the excited electron is injected to an oxidized state S^+ (at anode);

$$S^* \rightarrow S^+ + e^- \quad (2)$$

$$2S^{+}+3I^{-} \rightarrow 2S+I_3^{-} \quad (3)$$

3. the injected electron passes through the porous nanocrystalline material and reaches the transparent conducting oxide layer;
4. the electron is transferred to the triiodide in the electrolyte to yield iodine (at cathode);

$$I_3^{-}+2e^{-}(Pt)=3I^{-} \quad (4)$$

5. the reduction of the oxidized dye by the iodine in the electrolyte.

$$S^{+}+e^{-} \rightarrow S \quad (5)$$

hv is the photon energy; S stands for sensitizer; S*, electronically excited sensitizer; S^{+}, oxidized sensitizer.

4.4.2 Dye and efficiency

Different sensitizers have different transparency and absorbance on the sunlight spectral region. In dye solar cells, the dye is one of the key components for high power conversion efficiencies. Since highly efficient dye-sensitized solar cells (DSSCs) were first reported by Grätzel, substantial research has been carried out in the engineering of novel dye structures in order to enhance the performance of the system. At least 80 groups attended this research. The energy conversion efficiencies have been achieved over 10%.

Scientifically, a DSSC can achieve efficiency as high as 15% or more (Grätzel, 2003; Kroon et al., 2007). But till now, the highest efficiency is around 12%. This means there is a high potential for improvement in efficiency. The efficiency (η) is the function of the open circuit voltage (V_{oc}), the short circuit current (J_{sc}) and Fill factor (FF). The limitation of efficiency is on the three parts (Kroon et al., 2007):

a. Inefficient light absorption by existing sensitizer dyes in whole sunlight spectrum. Some are sensitized on UV-visible region but insensitive on IR region; some are sensitized on IR region, but insensitive on UV-visible region.
b. Sub-optimum photovoltage output. The improvements in the photovoltage could substantially increase device efficiencies by up to 50%.
c. Fill factors (FF) are limited in general by series resistance losses, light-intensity dependent recombination, non-ideal dark diode currents and, in some cases, shunt resistance losses.

Table 4.4 provides a summary of the best performance data obtained (state of the art) to date in solar light conversion, as well as open circuit voltages (V_{OC}) at various fill factors (FF) using various dyes for a number of surface areas.

In the new reports from M. Graetzel, EPFL has got very high efficiencies about sensitizers of C101 (11.3%, Thampi et al., 2008) and Z991 (11.91% (Grätzel, 2008),12.3% (Grätzel, 2009). There are still a lot of work to do to achieve the theory efficiency 15% (Kroon et al., 2007).

Many different dyes with a variety of chromophoric ligands have been synthesized and studied in DSSCs: polypyridine complexes of transition metals, metalloporphyrins, and metallo-phathalocyanines as well as different metal-free, donor-acceptor type dyes (Kalyanasundaram & Grätzel 2009). In most of the experiments, Ruthenium-based dyes are the main sensitizers. They are the best choices for DSSCs. They includesN3, N719, N749 (Black dye), N621 (η=9.57%, (Nazeeruddin et al., 2005), C104, Z907 (η=9.5%, Kalyanasundaram & Grätzel 2009) etc.

Sensitizer	Efficiency (%)	Voc (mv)	Jsc (mA/cm2)	FF (%)	Area (cm2)	research institution	Reference
N3	7.12-7.9				0.5	EPFL	O'Regan & Grätzel 1991
N3	10	720	18.2	73	0.31	EPFL	Nazeeruddin et al., 1993
N749	10.4	720	20.5	70	0.18	EPFL	Nazeeruddin et al., 2001
N3	9.3	770	16.8	72	1	EPFL	Nazeeruddin et al., 2003
N3	11.04	840	16.8	79		EPFL	Grätzel, 2004
Z910	10.2	777	17.2	76.4		EPFL	Wang et al., 2004
N719	11.18	846	17.7	75	0.16	EPFL	Nazeeruddin et al., 2005
N749	11.1	736	20.9	72.2	0.22	Sharp	CHIBA et al., 2006
N719	10.8	760	17.3	76	0.25	AIST	Chiba et al., 2006
N719	10.1	826	17	72	1.31	EPFL	Kroon et al., 2007
K77	10.5	780	19.2	72.5	0.158	EPFL	Kuang et al., 2007
C104	10.53	760	17.87	77.6	0.158		Gao et al., 2008

EPFL: Ecole Polytechnique Federale de Lausanne
AIST: the National Institute of Advanced Industrial Science and Technology (Japan)

Table 4.4 High efficiencies dye-sensitized solar cells development

N3 dye is one of the most commonly used sensitizing dyes for high-performance DSSCs. N719 dye is one of its derivatives,in which two protons are replaced by tetrabutylammonium cations (TBA) (figure 4.14). Both N3 and N719 have very good absorbance in UV-visible spectrum region, and can reach very high solar-energy-to-electricity-conversion efficiency (table 4.4). N749 (black dye) is sensitive in the low-frequency range of red and IR light.
Figure 4.15 and Table 4.5 show the structures and compositions of some of these high performance dyes respectively.
Recently some organic dyes have been developed. For example the D205 indoline dye (Ito et al., 2008) and C217 (Zhang et al., 2009) achieved efficiencies 9.5% and 9.8%, respectively.

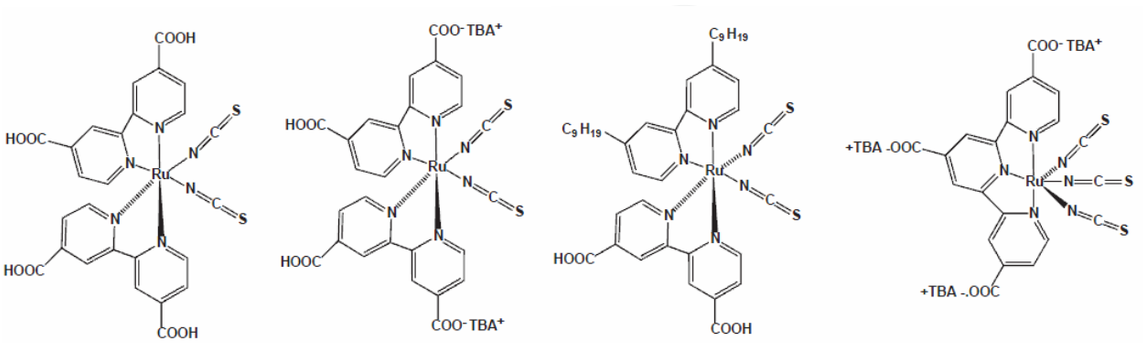

N3	N719	Z907	Black dye (N749)
η= 11.04%	η= 11.18%	η= 9.5%	η= 11.1%

Fig. 4.15. Structures of some of the most efficient Ru-based DSSCs

Dye	Name
N3	cis-bis(isothiocyanato)bis(2,2′-bipyridil-4,4′-dicarboxylate) ruthenium(II)
N719	cis-bis(isothiocyanato)bis(2,2′-bipyridyl-4,4′-dicarboxylate) ruthenium(II) bis-tetra-n-butylammonium
N621	cis-bis(isothiocyanato)(2,2′-bipyridyl-4,4′-dicarboxylate)(4,4′-ditridecyl-2,2′-bipyridine)ruthenium(II)
Z907	cis-bis(isothiocyanato)(2,2′-bipyridyl-4,4′-dicarboxylate)(4,4′-dinonyl-2,2′-bipyridine)ruthenium(II)
N749	tris(cyanato)-2,2',2″-terpyridyl-4,4',4″-tricarboxylate)Ru(II)

Table 4.5. Some dyes' compositions

4.4.3 Metal oxides

Semiconductor oxides used in dye-sensitized solar cell include TiO_2, ZnO, SnO_2, Nb_2O_5 etc., which serve as the carrier for the monolayers of the sensitizer using their huge surface and the medium of electron transfer to the conducting substrate. Anders Hagfeldtt et al (Hagfeldtt & Grätzel., 1995) even introduced nano-crystalline CdSe, CdS, WO_3, Fe_2O_3, In_2O_3 and Ta_2O_5 etc as the semiconductor oxides on the DSSC applications. Conventional high efficiency DSSC uses nano-crystalline TiO_2 as the semiconductor because TiO_2 has the properties such as low-cost price, abundance in the market, nontoxicity etc. ZnO has an energy gap of 3.37 eV, nearly identical to that of TiO_2. DSSCs built from ZnO nanoparticles show the second highest efficiencies after TiO_2. Karin Keis et al (Keis et al., 2002) developed a DSSC solar cell with nanoporous ZnO as the semiconductor to replace TiO_2 and N3 as the sensitizer. By improving the interfacial contact between dyes and ZnO particles in the film, overall solar-to-electric energy conversion efficiencies of up to 5% were obtained. Ming-Hong Lai et al (Lai et al., 2010) developed a new structure DSSC solar cell using ZnO to replace TiO_2. In this structure, a ZnO thin film is used as the TCO and a ZnO nanorod layer as semiconductor. There are also a lot of research about ZnO-based DSSC (Hongsith & Choopun., 2010; Martinson et al., 2007). Unfortunately, the ZnO-based DSSC efficiency is much lower compared to that based on TiO_2. One of the reasons for the low efficiency of ZnO-based DSSCs is the excessive dye aggregation on the ZnO surface, which in turn causes slower electron injection from the dye to ZnO (Zhang et al., 2008). The conditions as SnO_2 and other semiconductors are same low efficiencies. Up to date Nano-porous TiO_2 is still the best choice in semiconductor.

4.4.4 Electrolytes

The electrode in DSSC is to transport the charge carrier between photoanode and counter electrode. In the DSSC working cycle, the dye releases the electrons excited by the incident light into the conduction band of TiO_2. The dye loses electrons and must be reduced to its ground state rapidly. The ionic electrolyte must send electrons to the dye quickly. So, the electrode should have very good conductivity and good interfacial contact with the porous nanocrystalline layer and the counter electrode.

The electrolyte mixtures used in high-efficiency DSSC cells include liquid, solid-state and quasi-solid-state electrolytes.

Liquid electrolyte is widely used in DSSC. Most experiments of DSSC use liquid electrolyte including I^- / I_3^- redox couple. The light-to-electricity conversion efficiency based on I^- / I_3^- redox couple liquid electrolyte has been achieved to over 12%. This is the most efficient electrolyte. But the problem about this electrolyte is the corrosion for metals, which can cause sealing and long-time stability. Other kind redox couples such as Br^-/Br_2, SCN^-/SCN_2, $SeCN^-/SeCN_2$ also can be used in liquid electrolyte, but the light-to-electricity conversion efficiency is low. The limitations of liquid electrolyte are leakage of device, volatilization of organic solvents and long term stability. Solid-state electrolytes with no liquid materials can overcome the disadvantage of fluidity and volatility for liquid electrolytes and has long term stability. But the light-to-electricity conversion efficiency of DSSC with solid-state electrolytes is very low because of poor interface contact property and lower conductivity (Wu et al., 2008). Quasi-solid-state electrolyte is between liquid electrolyte and solid-state electrolyte. It has better long-term stability than liquid electrolytes but less than that of solid-state electrolyte. It has better ionic conductivity and interfacial contact property than that of solid-state electrolyte, but not as good as that of liquid electrolyte. Now DSSCs based on quasi-solid-state electrolyte are attracting more interest. Some researches got good results and the light-to-electricity conversion efficiencies are very high, such as 6.9% (Stathatos & Lianos., 2007) and 7.3% (Sathiya Priya et al., 2008). Compared with liquid electrolyte based DSSCs, the efficiencies of quasi-solid-state based DSSCs are very low.

4.4.5 Tandem-structure and dye-bilayer structure DSSC

Up to date, no sensitizer has good incident absorbance along the whole sunlight spectrum. Like conventional solar cell, the DSSC also can be synthesized as tandem-structure. But DSSC has special property that the nanocrystalline dye-sensitized solar cell DSSC can be designed by appropriate choice of the sensitizer to absorb incident photons in selective spectral regions of the solar spectrum while maintaining high transparency in the remaining wavelength range (Liska et al., 2006). So, in the tandem-structure DSSC, just choosing different sensitizers which have different transparency and absorbance on the sunlight spectral region to make top and bottom cells can get high conversion efficiencies. For example, Yanagida et al in AIST group developed a kind of DSSC tandem-structure dye-sensitized solar cell (Yanagida et al., 2010). N719 is sensitized on UV-visible region and N749 (black dye) is sensitized near infrared region (figure 4.16). The spectral response of the two systems is complementary to each other and reveals the advantage of employing them in a tandem mode. Tandem-structure DSSC with N719 as top cell and N749 as bottom cell sensitized on incident light from UV to infrared region can reach the highest photovoltaic conversion efficiency of 10.6% (parallel structure) under solar-simulating light conditions (AM1.5, 100mWcm^{-2}).

A DSSC cell can combine a CIGS cell to buildup a tandem-structure cell. Liska et al developed a photovoltaic tandem cell comprising a nanocrystalline dye-sensitized solar cell (N719 based) as a top cell for high-energy photons and a copper indium gallium selenide (CIGS) thin-film bottom cell for lower-energy photons (Liska et al., 2006). Figure 4.17 shows photon-to-current conversion efficiency (IPCE) of this DSSC/CIGS tandem-structure solar cell. The DSSC top cell shows a strong response in the UV, blue, and green wavelength domains and the CIGS bottom

cell exhibits high external quantum efficiencies in the red and near IR parts of the spectrum extending from 700 to 1150 nm where the DSSC is insensitive to light. This DSSC/CIGS tandem-structure is sensitized on the spectrum from UV to IR region.

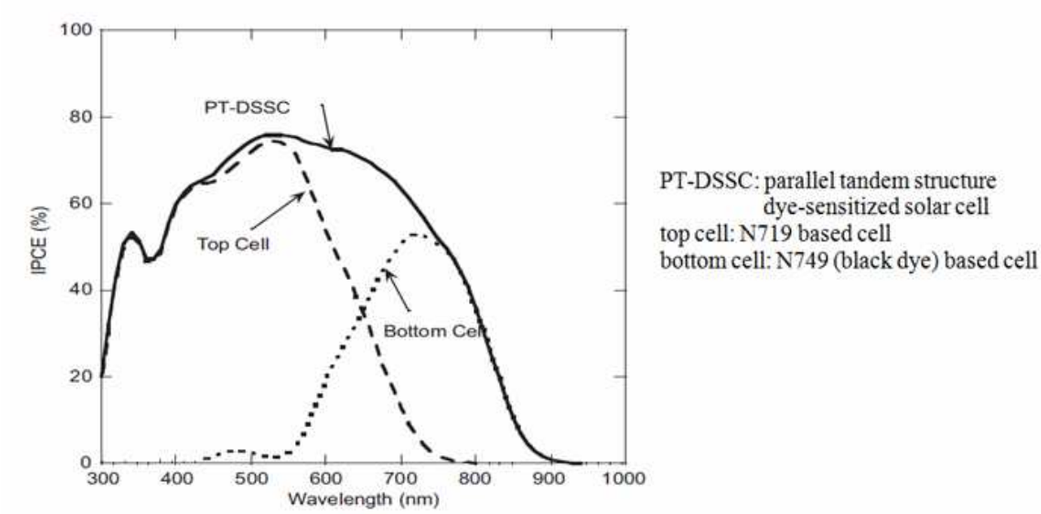

Fig. 4.16. The incident monochromatic photon-to-current conversion efficiency (IPCE) spectra of a PT-DSSC (solid line) and its top and bottom cells (dashed and dotted lines, respectively).

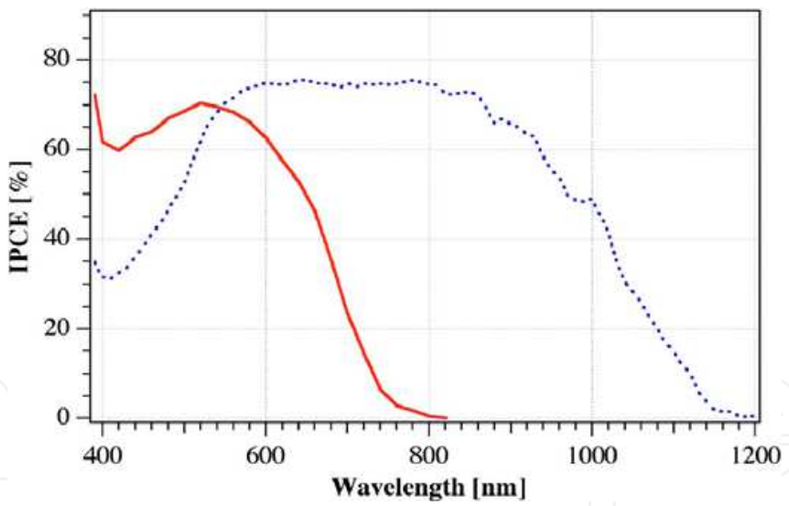

Fig. 4.17. Spectral response curves of the photon-to-current conversion efficiency (IPCE) for a DSSC top cell (bold line) and a CIGS bottom cell (dotted line) (Liska et al., 2006)

This cell can achieve photovoltaic conversion efficiencies as high as 15.75% which was significantly higher than that of the individual cells. Here the N719 based DSSC top cell efficiency is 7.85% and the CIGS bottom cell efficiency is 8.17%.

Inakazu et al studied a dye-sensitized solar cells (DSSC) containing dye-bilayer structure of black dye and NK3705. This structure was fabricated by staining one TiO_2 layer with these two dyes, step by step. The short circuit current (J_{sc}) and the incident photon to current efficiency (IPCE) of this cell are almost the sum of those of DSSC stained with black dye only

and DSSC stained with NK3705 only. The efficiency of this dye-bilayer solar cell is 9.16%, which is higher than that of black-dye based solar cell (7.28%) and NK3705 based cell (1.85%) (Inakazu et al., 2008).

4.5 Polymer solar cells

A polymer solar cell is also called an organic solar cell or a plastic solar cell. The polymer as substrate can make the cell flexible. The polymer solar cell is typically made from a nanocomposite thin film material. Such a solar cell produces electricity from sunlight by the polymer. Compared with silicon-based solar cells, polymer solar cells can greatly lower the cost. For a polymer solar cell, there are three major ways to lower the cost. First, it uses low cost plastic as the active materials to convert solar energy into electricity; second, the active plastic layer thickness is in nano-scale, this means the raw materials consumption will be significantly decreased; the third aspect is the low manufacturing cost, the solution processing is low easy and low cost. The ink-jet printing, micro-contact printing, and other soft lithography techniques have further improved the potential of conjugated polymers for low-cost fabrication of large-area integrated devices on both rigid and flexible substrates. These techniques are similar to printing on newspaper and the cost is very low. Polymer solar cells is cheaper to make than thin-film cadmium-telluride (CdTe) or copper indium gallium selenide (CIGS) ones because they use low-cost materials and are easy to print. The main reason for the extensive interest in polymer semiconducting materials is their potential for the realization of a low cost, easily processed, light-weight and mechanical flexible device. The main problems of polymer solar cell are photochemical degradation and low light-electric conversion efficiency. The research of polymer solar cells concentrates on increasing photochemical stability and energy conversion efficiency.

4.5.1 Structure of polymer solar cell

Figure 4.18 shows the polymer solar cell structure. It is similar with CdTe, CIGS and DSSC. The difference is the active layer. It is polymer blend, including a p-type semiconductor (donor) and an n-type semiconductor (acceptor). The basic process includes absorption of light, charge transfer and separation of the opposite charges, charge transport and charge collection. The process is the same with DSSC. So, it can also be classified as dye-sensitized solar cell.

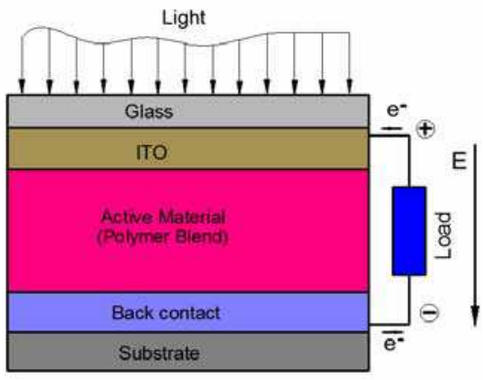

4.18. Typical polymer solar cell structure

Donors:
MDMO-PPV = poly[2-methoxy-5-(3´,7´-dimethyloctyloxy)-p-phenylene vinylene];
P3HT= poly(3-hexylthiophene);
PFDTBT: poly[2,7-[9-(2´-ethylhexyl)-9- hexylfluorene]-alt-5,5-(4´,7´-di-2-thienyl-2´,11´,3´-benzothiadiazole)].
Acceptors:
PCBM: 3´-phenyl-3´H-cyclopropa[1,9][5,6]fullerene-C60-Ih-3´-butanoic acid methyl ester;
PCBM: 3´-phenyl-3´H-cyclopropa[8,25][5,6]fullerene-C70-D5h(6)-3´-butanoic acid methyl ester.

4.5.2 Efficiency

Due to the inferior charge-transport properties and limited spectral absorption range of the polymer active layer, the overall power conversion efficiencies (PCE) reported are still low. Green et al have reported the high efficiencies polyer solar cells. For single solar cell, the efficiency is 5.15% (Voc, 876mV; Jsc, 9.39mA/cm2; FF, 62.5%). For 2-cell tandem solar cell, the efficiency is 6.1% (Voc, 1589mV; Jsc, 6.18mA/cm2; FF, 61.9%) (Green et al., 2010). This low efficiency limits the application of commercialization. Solarmer Energy, Inc is the leading developer company in polymer solar cell technology. In 2009 alone, Solarmer produced three certified world records: 6.8%, 7.6% and 7.9%. Recently a new world record of 8.13% for their organic photovoltaic (OPV) cell efficiency was achieved, which was certified by the National Renewable Energy Laboratory (NREL). (http://www.solarmer.com). This new development made the commercialization of polymer solar cells is possible. This cutting-edge technology has the potential to drive energy production cost down to 12-15 cents/kWh. But for polymer solar cell, the efficiency over 15% can have a major impact on the solar cell power market. In theory, the efficiency with 15-20% is possible. This means there is still much work to do to improve the efficiency.

5. Summery and conclusions

Based on the review of thin film typed nanocomposites for solar energy conversion, the following conclusions may be made. Various nanocomposite thin films for solar cell fabrication are still under development. The principle of photovoltaic energy conversion of nanocomposites is different from that of the first generation of solar cells, i.e. silicon cells because of the structure complexity. The efficiency of solar cells could potentially be improved by using two dimensional nanocomposite cells such as $CuInGaSe_2$(CIGS), dye-sensitized solar cell (DSSC). There are many challenges in polymer based solar cells research because they have very low efficiencies.

6. Reference

AbuShama, J. A., Johnston, S., Moriarty, T., Teeter, G., Ramanathan, K., & Noufi, R. (2004). Properties of ZnO/CdS/$CuInSe_2$ Solar Cells with Improved Performance. *Prog. Photovolt: Res. Appl. , 12*, pp.39–45.

AbuShama, J., Noufi, R., & Johnston, S. (2004). Improved Performance in $CuInSe_2$ and Surface-Modified $CuGaSe_2$ Solar Cells. *the 2004 DOE Solar Energy Technologies, Program Review Meeting*. Denver, Colorado.

Anderson, T., Crisalle, O., Li, S., & Holloway, P. (2003). *Future CIS Manufacturing Technology Development.* Gainesville, Florida.

Aramoto, T., Adurodija, F., Nishiyama, Y., Arita, T., Hanafusa, A., Omura, K.,& Morita, A. (2003). A new technique for large-area thin film CdS/CdTe solar cells. *Solar Energy Materials & Solar Cells , 75*, pp. 211–217.

Barri, K. J., & Ferekides, C. (2005). INTRODUCTION OF Cu IN CdS AND ITS EFFECT ON CdTe SOLAR CELLS. *31st IEEE Photovoltaic Specialists Conference.*

Beecroft, L. L., & Ober., C. K. (1997). Nanocomposite Materials for Optical Applications. *Chem. Mater. , 9*, 1302-1317.

Bhattacharya, R., Balcioglu, A., & Ramanathan, K. (2001). Deep-level transient spectroscopy (DLTS) of CdS/$CuIn_{(1-x)}Ga_xSe_2$-based solar cells prepared from electroplated and autoplated precursors, and by physical vapor deposition. *Thin Solid Films , 384*, pp. 65-68.

Britta, J., & Ferekides, C. (1993). Thin-film Cd/CdTe solar cell with 15.8% efficiency. *Appt. Phys. Lett. , 62* (22), 2851-2852.

Castillo-Alvarado, F., Inoue-Chávez, J., Vigil-Galán, O., Sánchez-Meza, E., López-Chávez, E., & Contreras-Puente, G. (2010). C–V calculations in CdS/CdTe thin films solar cells. *Thin Solid Films , 518*, 1796–1798.

Chen, Z., Tang, Y., Zhang, L., & Luo, L. (2006). Electrodeposited nanoporous ZnO films exhibiting enhanced performance in dye-sensitized solar cells. *Electrochimica Acta , 51*, 5870–5875.

Chiba, Y., Islam, A., Komiya, R., Koide, N., & Han, L. (2006). Conversion efficiency of 10.8% by a dye-sensitized solar cell using a TiO_2 electrode with high haze. *Appl. Phys. Lett. , 88*, 223505 1-3.

CHIBA, Y., ISLAM, A., WATANABE, Y., KOMIYA, R., KOIDE, N., & HAN, L. (2006). Dye-Sensitized Solar Cells with Conversion Efficiency of 11.1%. *Japanese Journal of Applied Physics , 45* (25), L638–L640.

Chu, T. L., Chu, S. S., Ferekides, C., Wu, C. Q., Britt, J., & Wang, C. (1991). 13.4% efficient thin-film CdS/CdTe solar cells. *J. Appl. Phys. , 70* (12), pp. 7608-7612.

Colombo, E. B., Calusi, S., Giuntini, L., Lo Giudice, A., Manfredotti, C., Massi, M., Olivero, P., Romeo, A., Romeo, N. & Vittone E. (2009). IBIC analysis of CdTe/CdS solar cells. *Nuclear Instruments and Methods in Physics Research B , 267*, pp. 2181–2184.

Compaan, A. D., Gupta, A., Drayton, J., Lee, S.-H., & Wang, S. (2004). 14% sputtered thin-film solar cells based on CdTe. *phys. stat. sol. (b) , 241* (3), pp. 779–782.

Compaan, A. D., Gupta, A., Lee, S., Wang, S., & Drayton, J. (2004). High efficiency, magnetron sputtered CdS/CdTe solar cells. *Solar Energy , 77*, pp. 815–822.

Contreras Puente, G., Vigil, O., Ortega-LoÂpez, M., Morales-Acevedo, A., Vidal, J., & Albor-Aguilera, M. (2000). New window materials used as heterojunction partners on CdTe solar cells. *Thin Solid Films , 361-362*, 378-382.

Contreras, M. A., Egaas, B., Ramanathan, K., Hiltner, J., Swartzlander, A., Hasoon, F., & Noufi, R. (1999). Progress Toward 20% Efficiency in Cu(In,Ga)Se_2 Polycrystalline Thin-film Solar Cells. *Prog. Photovolt: Res. Appl. , 7*, pp.311-316.

Contreras, M. A., Ramanathan, K., AbuShama, J., Hasoon, F., Young, D. L., Egaas, B., & Noufi, R. (2005). Diode Characteristics in State-of-the-Art ZnO/CdS/Cu($In_{1-x}Ga_x$)Se_2 Solar Cells. *Prog. Photovolt: Res. Appl. , 13*, 209–216.

Contreras, M. A., Romero, M. J., To, B., Hasoon, F., Noufi, R., Ward, S., & Ramanathan, K. (2002). Optimization of CBD CdS process in high-efficiency Cu(In,Ga)Se_2-based solar cells. *Thin Solid Films , 403-404*, 204-211.

Contreras, M., Nakada, T., Hongo, M., Pudov, A., & Sites, J. (2003). ZnO/ZnS(O,OH)-/Cu(In,Ga)Se_2/Mo SOLAR CELL WITH 18.6% EFFICIENCY. *Proceedings 3rd World Conference of Photovoltaic Energy Conversion*, (pp. 570-573). Osaka, Japan.

Delahoy, A. E., Chen, L., Akhtar, M., Sang, B., & Guo, S. (2004). New technologies for CIGS photovoltaics. *Solar Energy , 77*, pp. 785–793.

Dhere, N. G. (2006). Present status and future prospects of CIGSS thin film solar cells. *Solar Energy Materials & Solar Cells , 90*, pp.2181–2190.

Dhere, N. G. (2006). Present status and future prospects of CIGSS thin film solar cells. *Solar Energy Materials & Solar Cells , 90*, 2181-2190.

Dhere, R., Rose, D., Albin, D., Asher, S., Al-Jassim, M., Cheong, H., Swartzlander, A., Moutinho, H., Coutts, T. & Sheldon, P. (1997). Influence of CdS/CdTe Interface Properties on the Device Properties. *the 26th IEEE Photovoltaic Specialists Conference.* Anaheim, California.

Dobson, K. D., Visoly-Fisher, I., Hodes, G., & Cahen, D. (2000). Stability of CdTe/CdS thin-film solar cells. *Solar Energy Materials & Solar Cells , 62*, pp. 295-325.

Dobson, K. D., Visoly-Fisher, I., Hodes, G., & Cahen, D. (2000). Stability of CdTe/CdS thin-film solar cells. *Solar Energy Materials & Solar Cells , 62*, 295-325.

Dzhafarov, T., Yesilkaya, S., Yilmaz Canli, N., & Caliskan, M. (2005). Diffusion and influence of Cu on properties of CdTe thin films and CdTe/CdS cells. *Solar Energy Materials & Solar Cells , 85*, 371–383.

Ennaoui, A., Siebentritt, S., Lux-Steiner, M., Riedl, W., & Karg, F. (2001). High-effciency Cd-free CIGSS thin-film solar cells with solution grown zinc compound buffer layers. *Solar Energy Materials & Solar Cells , 67*, 31-40.

Enrıquez, J., Pantoja, E., Barojas, G., Silva Gonzalez, R., & Pal, U. (2007). S and Te inter-diffusion in CdTe/CdS hetero junction. *Solar Energy Materials & Solar Cells , 91*, pp. 1392–1397.

Eze, F., & Okeke, C. (1997). Chemical-bath-deposited cobalt sulphide film: preparation effects. *Materials Chemistry and physics , 47*, 31-36.

Fahrenbruch, A. L. (2007). Exploring Back Contact Technology to Increase CdS/CdTe Solar Cell Efficiency. *the Materials Research Society Meeting*, (pp. Y7-5). San Francisco, CA.

Ferekides, C., Marinskiy, D., Viswanathan, V., Tetali, B., Palekis, V., Selvaraj, P., & Morel, D. L. (2000). High efficiency CSS CdTe solar cells. *Thin Solid Films , 361-362*, pp. 520-526.

Gabor, A. M., Tuttle, J. R., Albin, D. S., Contreras, M. A., Noufi, R., & Hermann, A. M. (1994). High-efficiency $CuIn_xGa_{1-x}Se_2$ solar cells made from $(In_x,Ga_{1-x})_2Se_3$ precursor films. *Appl. Phys. Lett. , 65* (2), 198-200.

Gamboa, S., Sebastian, P., Mathew, X., Nguyen-Cong, H., & Chartier, P. (1999). A CdTe/PMeT photovoltaic structure formed by electrodeposition and processing. *Solar Energy Materials & Solar Cells , 59*, 115-124.

Gao, F., Wang, Y., Zhang, J., Shi, D., Wang, M., Humphry Baker, R., Wang, P., Zakeeruddin, S. M. & Grätzel, M. (2008). A new heteroleptic ruthenium sensitizer enhances the absorptivity of mesoporous titania film for a high efficiency dye-sensitized solar cell, Chem. Commun., 2008, 2635–2637.

Gayam, S., Bapanapalli, S., Zhao, H., Nemani, L., Morel, D., & Ferekides, C. (2007). The structural and electrical properties of Zn–Sn–O buffer layers and their effect on CdTe solar cell performance. *Thin Solid Films , 515*, 6060-6063.

Grätzel, M. (2009). The Advent of Mesoscopic Solar Cells. *International Symposium on Innovative Solar Cells 2009.* Tokyo, Japan.

Grätzel, M. (2004). Conversion of sunlight to electric power by nanocrystalline dye-sensitized solar cells. *Journal of Photochemistry and Photobiology A: Chemistry , 164*, 3-14.

Grätzel, M. (2003). Dye-sensitized solar cells. *Journal of Photochemistry and Photobiology C: Photochemistry Reviews , 4*, 145-153.

Grätzel, M. (2008). Power from the Sun, The advent of mesoscopic solar cells. *International Symposium on Solar Cells and Solar Fuels.* Dalian, China.

Grätzel, M. (2009). Recent Advances in Sensitized Mesoscopic Solar Cells. *ACCOUNTS OF CHEMICAL RESEARCH , 42* (11), 1788-1798.

Green, M. A., Emery, K., Hishikawa, Y., & Warta, W. (2010). Solar cell efficiency tables (version 35). *PROGRESS IN PHOTOVOLTAICS: RESEARCH AND APPLICATIONS, 18*, 144-150.

Guillemoles, J.-F., Kronik, L., Cahen, D., Rau, U., Jasenek, A., & Schock, H.-W. (2000). Stability Issues of Cu(In,Ga)Se2-Based Solar Cells. *J. Phys. Chem. , B* (104), 4849-4862.

Gupta, A., & Compaan, A. D. (2004). All-sputtered 14% CdS/CdTe thin-film solar cell with ZnO:Al transparent conducting oxide. *Appl. Phys. Lett. , 85* (4), pp. 684-686.

Gupta, A., Parikh, V., & Compaan, A. D. (2006). High efficiency ultra-thin sputtered CdTe solar cells. *Solar Energy Materials & Solar Cells , 90*, pp. 2263–2271.

Hagfeldtt, A., & Grätzel, M. (1995). Light-Induced Redox Reactions in Nanocrystalline Systems. *Chem, Rev. , 95*, 49-68.

Han, L., Fukui, A., Fuke, N., Koide, N., & Yamanaka, R. (2006). High Efficiency of Dye-Sensitized Solar Cell and Module. *Photovoltaic Energy Conversion, Conference Record of the 2006 IEEE 4th World Conference on*, *1*, pp. 179-182. Waikoloa, HI.

Hariskos, D., Spiering, S., & Powalla, M. (2005). Buffer layers in Cu(In,Ga)Se_2 solar cells and modules. *Thin Solid Films 480–481,* pp. 99– 109.

Hermanna, A., Gonzalez, C., Ramakrishnan, P., Balzar, D., Popa, N., Rice, P., Marshall, C. H., Hilfiker, J. N., Tiwald, T., Sebastian, P. J., Calixto, M. E. & Bhattacharya, R. N. (2001). Fundamental studies on large area Cu(In,Ga)Se_2 films for high efficiency solar cells. *Solar Energy Materials & Solar Cells , 70*, 345–361.

Hodes, G. (2003). *Chemical Solution Deposition of Semiconductor Films.* New York: Marcel Dekker, Inc.

Hongsith, N., & Choopun, S. (2010). ZnO Nanobelts as a Photoelectrode for Dye-Sensitized Solar Cell. *Chiang Mai J. Sci. , 37* (1), 48-54.

Huang, C., Meen, T., Lai, M., & Chen, W. (2004). Formation of $CuInSe_2$ thin films on flexible substrates by electrodeposition (ED) technique. *Solar Energy Materials & Solar Cells* , 553-565.

Hubert, C., Naghavi, N., Roussel, O., Etcheberry, A., Hariskos, D., Menner, R., Powalla, M., Kerrec, O. & Lincot, D. (2009). The Zn(S,O,OH)/ZnMgO Buffer in Thin Film $Cu(In,Ga)(S,Se)_2$ -Based Solar Cells Part I: Fast Chemical Bath Deposition of Zn(S,O,OH) Buffer Layers for Industrial Application on Co-evaporated $Cu(In,Ga)Se_2$ and Electrodeposited $CuIn(S,Se)_2$ Solar Cells. *Prog. Photovolt: Res. Appl. , 17*, 470-478.

Inakazu, F., Noma, Y., Ogomi, Y., & Hayase, S. (2008). Dye-sensitized solar cells consisting of dye-bilayer structure stained with two dyes for harvesting light of wide range of wavelength. *APPLIED PHYSICS LETTERS , 93*, 093304 1-3.

Ito, S., Miura, H., Uchida, S., Takata, M., Sumioka, K., Liska, P., Comte, P., Pechy, P. & Grätzel, M. (2008). High-conversion-efficiency organic dye-sensitized solar cells with a novel indoline dye. *Chem. Commun.* , 5194-5196.

Ivanov, V., Balakai, V., Kurnakova, N., Arzumanova, A., & Balakai, I. (2008). Synergistic Effect in Nickel–Teflon Composite Electrolytic Coatings. *Russian Journal of Applied Chemistry , 81* (12), 2169–2171.

Kalyanasundaram, K., & Grätzel, M. (2009). Efficient Dye-Sensitized Solar Cells for Direct Conversion of Sunlight to Electricity. *Material Matters , 4* (4), 88-90.

Kapur, V. K., Bansal, A., Le, P., & Asensio, O. I. (2003). Non-vacuum processing of $CuIn_{(1-x)}Ga_xSe_2$ solar cells on rigid and flexible substrates using nanoparticle precursor inks. *Thin Solid Films , 431–432*, 53-57.

Kato, K., Hibino, T., Komoto, K., Ihara, S., Yamamoto, S., & Fujihara, H. (2001). A life-cycle analysis on thin-film CdS/CdTe PV modules. *Solar Energy Materials & Solar Cells , 67*, pp. 279-287.

Kazmerski, L. (2004). Photovoltaics R&D: At the Tipping Point. *the 2004 DOE Solar Energy Technologies Program Review Meeting.* Denver, Colorado.

Keis, K., Magnusson, E., Lindstrom, H., Lindquist, S. E., & Hagfeldt, A. (2002). A 5% efficient photoelectrochemical solar cell based on nanostructured ZnO electrodes. *Solar Energy Materials & Solar Cells , 73*, 51-58.

Khrypunov, G., Romeo, A., Kurdesau, F., Batzner, D., Zogg, H., & Tiwari, A. (2006). Recent developments in evaporated CdTe solar cells. *Solar Energy Materials & Solar Cells , 90*, pp. 664–677.

King, R. (2009). Raising the Efficiency Ceiling in Multijunction Solar Cells. *Stanford Photonics Research Center Symposium.*

Kois, J., Ganchev, M., Kaelin, M., Bereznev, S., Tzvetkova, E., Volobujeva, O., Stratieva, N. & Tiwari, A. N. (2008). Electrodeposition of Cu–In–Ga thin metal films for Cu(In, Ga)Se2 based solar cells. *Thin Solid Films , 516*, 5948-5952.

Krishnan, S., Sanjeev, G., Pattabi, M., & Mathew, X. (2009). Effect of electron irradiation on the properties of CdTe/CdS solar cells. *Solar Energy Materials & Solar Cells , 93*, pp. 2–5.

Kroon, J. M., Bakker, N. J., Smit, H. J., Liska, P., Thampi, K. R., Wang, P., Zakeeruddin, S. M., Grätzel, M., Hinsch, A., Hore, S., Wu¨rfel, U., Sastrawan, R., Durrant, J. R., Palomares, E., Pettersson, H., Gruszecki, T., Walter, J., Skupien, K. & Tulloch, G. E. (2007). Nanocrystalline Dye-sensitized Solar Cells Having Maximum Performance. *Prog. Photovolt: Res. Appl. , 15*, 1–18.

Kuang, D., Klein, C., Ito, S., Moser, J.-E., Humphry-Baker, R., Evans, N., Duriaux, F., Grätzel, C., Zakeeruddin, S. M. & Grätzel, M. (2007). High-Efficiency and Stable Mesoscopic Dye-Sensitized Solar Cells Based on a High Molar Extinction Coefficient Ruthenium Sensitizer and Nonvolatile Electrolyte. *Adv. Mater. , 19*, 1133-1137.

Kumazawa, K., Shibutani, S., Nishio, T., Aramoto, T., Higuchi, H., Arita, T., Hanafusa, A., Omura, K., Murozono, M. & Takakura, H. 15.1% Highly efficient thin film CdS/CdTe Solar cell. *Solar Energy Materials and Solar , 49*, pp. 205-212.

Kylner, A. (1999). Effect of impurities in the CdS buffer layer on the performance of the Cu(In,Ga)Se_2 thin film solar cell. *J. Appl. Phys. , 85* (9), 6858-6865.

Lai, M. H., Tubtimtae, A., Lee, M. W., & Wang, G. J. (2010). ZnO-Nanorod Dye-Sensitized Solar Cells: New Structure without a Transparent Conducting Oxide Layer. *ZnO-International Journal of Photoenergy , 2010*.

Lee, J. (2005). Comparison of CdS films deposited by different techniques: Effects on CdTe solar cell. *Applied Surface Science , 252*, 1398–1403.

Levy-Clement, C., Katty, A., Bastide, S., Zenia, F., Mora, I., & Munoz-Sanjose, V. (2002). A new CdTe/ZnO columnar composite film for Eta-solar cells. *Physica , E* (14), 229-232.

Liska, P., Thampi, K. R., & Grätzel, M. (2006). Nanocrystalline dye-sensitized solar cell/copper indium gallium selenide thin-film tandem showing greater than 15% conversion efficiency. *APPLIED PHYSICS LETTERS , 88*, 203103 1-3.

Lu, C., Cui, Z., Wang, Y., Li, Z., Guan, C., Yang, B., & Shen, J. (2003). Preparation and characterization of ZnS–polymer nanocomposite films with high refractive index. *Journal of Materials Chemistry , 13*, 2189–2195.

Lu, H., Liu, Y., Gou, J., Leng, J., & Du, S. (2010). Synergistic effect of carbon nanofiber and carbon nanopaper on shape memory polymer composite. *APPLIED PHYSICS LETTERS , 96*, 084102 1-3.

Lundberg, O., Bodegard, M., Malmstrom, J., & Stolt, L. (2003). Influence of the Cu(In,Ga)Se_2 Thickness and Ga Grading on Solar Cell Performance. *Prog. Photovolt: Res. Appl., 11*, 77-88.

Lundberg, O., Edoff, M., & Stolt, L. (2005). The effect of Ga-grading in CIGS thin film solar cells. *Thin Solid Films , 480-481*, 520-525.

Luschitz, J., Siepchen, B., Schaffner, J., Lakus-Wollny, K., Haindl, G., Klein, A., et al. (2009). CdTe thin film solar cells: Interrelation of nucleation, structure and performance. *Thin Solid Films , 517*, 2125–2131.

Marayanan, K., Vijayakumar, K., Mnair., K., & Nrao, G. (1997). Chemical bath deposition of CdS thin films and their partial conversion to CdO on annealing. *Bull. Mater. Sci. , 20* (3), pp. 287-295.

Marsillac, S., Parikh, V., & Compaan, A. (2007). Ultra-thin bifacial CdTe solar cell. *Solar Energy Materials & Solar Cells , 91*, pp. 1398–1402.

Martinson, A. B., Elam, J. W., Hupp, J. T., & Pellin, M. J. (2007). ZnO Nanotube Based Dye-Sensitized Solar Cells. *Nano Lett. , 7* (8), 2183-2187.

Mathew, X., J. Enriquez, P., Romeo, A., & Tiwari, A. N. (2004). CdTe/CdS solar cells on flexible substrates. *Solar Energy , 77*, pp. 831–838.

Mathew, X., Sebastian, P., Sanchez, A., & Campos, J. (1999). Structural and optoelectronic properties of electrodeposited CdTe on stainless steel foil. *Solar Energy Materials & Solar Cells , 59*, 99-114.

Matsune, K., Oda, H., Toyama, T., Okamoto, H., Kudriavysevand, Y., & Asomoza, R. (2006). 15% Efficiency CdS/CdTe thin film solar cells using CdS layers doped with metal organic compounds. *Solar Energy Materials & Solar Cells , 90*, pp. 3108-3114.

Matulionis, I., Sijin, H., Drayton, J., Price, K., & Compaan, A. (2001). Cadmium telluride solar cells on molybdenum substrates. *In Proceedings of the Materials Research Society symposium on II–VI compound semiconductor photovoltaic materials.* Warrenda, PA.

Mendoza-Perez, R., Sastre-Hernandez, J., Contreras-Puente, G., & Vigil-Galan, O. (2009). CdTe solar cell degradation studies with the use of CdS as the window material. *Solar Energy Materials & Solar Cells , 93*, 79-84.

Meyer, G., & Saura, J. (1992). CdTe crystals grown by chemical vapour deposition. *Journal of materials science letters , 11*, 143-144.

Minami, T. (2008). Present status of transparent conducting oxide thin-film development for Indium-Tin-Oxide (ITO) substitutes. *Thin Solid Films , 516*, 5822–5828.

Minami, T. (2005). Transparent conducting oxide semiconductors for transparent electrodes. *Semicond. Sci. Technol. , 20*, pp. S35–S44.

Mitchell, K. W., Fahrenbruch, A. L., & Bube, R. H. (1977). Evaluation of the CdS/CdTe heterojunction solar cell. *J. Appl. Phys. , 48* (10), pp. 4365-4371.

Morales-Acevedo, A. (2006). Can we improve the record efficiency of CdS/CdTe solar cells? *Solar Energy Materials & Solar Cells , 90*, 2213–2220.

Moutinho, H., Dhere, R., Romero, M., Jiang, C.-S., To, B., & Al-Jassim, M. (2008). RECRYSTALLIZATION OF PVD CdTe THIN FILMS INDUCED BY $CdCl_2$ TREATMENT–A COMPARISON BETWEEN VAPOR AND SOLUTION PROCESSES. *the 33rd IEEE Photovoltaic Specialists Conference* . San Diego, California.

Naghavi, N., Spiering, S., Powalla, M., Cavana, B., & Lincot, D. (2003). High-Efficiency Copper Indium Gallium Diselenide (CIGS) Solar Cells with Indium Sulfide Buffer Layers Deposited by Atomic Layer Chemical Vapor Deposition (ALCVD). *Prog. Photovolt:Res. Appl. , 11*, pp. 437–443.

NAKADA, T., & MIZUTANI, M. (2002). 18% Efficiency Cd-Free Cu(In, Ga)Se_2 Thin-Film Solar Cells Fabricated Using Chemical Bath Deposition (CBD)-ZnS Buffer Layers. *Jpn. J. Appl. Phys. , 41*, pp. L 165–L 167.

Nazeeruddin, M. K., Angelis, F. D., Fantacci, S., Selloni, A., Viscardi, G., Liska, P., Ito, S., Takeru, B. & Grätzel, M. (2005). Combined Experimental and DFT-TDDFT Computational Study of Photoelectrochemical Cell Ruthenium Sensitizers. *J. AM. CHEM. SOC. , 127*, 16835-16847.

Nazeeruddin, M. K., Humphry Baker, R., Liska, P., & Grätzel, M. (2003). Nazeeruddin, Md. K.; HumphrInvestigation of Sensitizer Adsorption and the Influence of Protons on Current and Voltage of a Dye-Sensitized Nanocrystalline TiO_2 Solar Cell.

Nazeeruddin, Md. K.; Humphry-Baker, R.; Liska, P. ; Grätzel, M. (2003). Investigation of Sensitizer Adsorption and the InfluencJ. Phys. Chem. B , 8981-8987.

Nazeeruddin, M. K., Kay, A., Rodicio, l., Humpbry-Baker, R., Miiller, E., Liska, P., Vlachopoulos, N. & Grätzel, M. (1993). Conversion of Light to Electricity by cis-XzBis (2,2'-bipyridyl-4,4'-dicarboxylate)ruthenium(11), Charge-Transfer Sensitizers (X=Cl^-, Br^-,I^-,CN^-, and SCN^-) on Nanocrystalline TiO_2 Electrodes. *J. Am. Chem. SOC. , 115*, 6382-6390.

Nazeeruddin, M. K., Pechy, P., Renouard, T., Zakeeruddin, S. M., Humphry-Baker, R., Comte, P., Liska, P., Cevey, L., Costa,E., Shklover, V., Spiccia, L., Deacon, G. B., Bignozzi, C. A. & Grätzel, M. (2001). Engineering of Efficient Panchromatic Sensitizers for Nanocrystalline TiO2-Based Solar Cells. *J. Am. Chem. Soc. , 123*, 1613-1624.

Negami, T., Aoyagi, T., Satoh, T., Shimakawa, S. i., Hayashi, S., & Haskimoto, Y. (2002). Cd free CIGS solar cells fabricated by dry processes. *Photovoltaic Specialists Conference, 2002. Conference Record of the Twenty-Ninth IEEE*, (pp. 656-659).

Noufi, R. (2006). High Efficiency CdTe and CIGS Thin Film Solar Cells: Highlights of the Technologies Challenges. *the 2006 IEEE 4th World Conference on Photovoltaic Energy Conversion (WCPEC-4)*. Waikoloa, Hawaii.

Ochoa-Landın, R., Vigil-Galan, O., Vorobiev, Y., & Ramırez-Bon, R. (2009). Chemically deposited Te layers improving the parameters of back contacts for CdTe solar cells. *Solar Energy , 83*, 134-138.

Ohashi, D., Nakada, T., & Kunioka, A. (2001). Improved CIGS thin-film solar cells by surface sulfurization using In_2S_3 and sulfur vapor. *Solar Energy Materials & Solar Cells , 67*, pp. 261-265.

Okamoto, T., Yamada, A., & Konagai, M. (2000). Optical and electrical characterizations of highly efficient CdTe thin film solar cells prepared by close-spaced sublimation. *Journal of Crystal Growth , 214/215*, pp. 1148-1151.

O'Regan, B., & Gratzel, M. (1991). A low-cost, high-efficiency solar cell based on dye-sensitized colloidal TiO2 films. *Nature , 353*, 737-740.

Pantoja Enriquez, J., Mathew, X., Hernandez, G., Pal, U., Magana, C., Acosta, D. R., Guardian, R., Toledo, J. A., Contreras Puente, G. & Chavez Carvayar, J. A. (2004). CdTe/CdS Solar cells on flexible molybdenum substrates. *Solar Energy Materials & Solar Cell , 82*, 307-314.

Peter, L., & Wang, R. L. (1999). Channel flow cell electrodeposition of CdTe for solar cells. *Electrochemistry Communications , 1*, 554–558.

Pinheiro, W. A., Falcão, V. D., Cruz, L. R., & Ferreira, C. L. (2006). Comparative Study of CdTe Sources Used for Deposition of CdTe Thin Films by Close Spaced Sublimation Technique. *Materials Research , 9* (1), pp. 47-49.

Ramanathan, K., Contreras, M. A., Perkins, C. L., Asher, S., Hasoon, F. S., Young, D., Romero, M., Metzger, W., Noufi, R., Ward, J. & Duda, A. (2005). Properties of 19.2% Efficiency ZnO/CdS/$CuInGaSe_2$ Thin-film Solar Cells. *Prog. Photovolt: Res. Appl. , 11*, 225-230.

Repins, I., Contreras, M. A., Egaas, B., DeHart1, C., Scharf, J., Perkins, C. L., To, B. & Noufi, R. (2008). 19.9%-efficient ZnO/CdS/$CuInGaSe_2$ Solar Cell with 81.2% Fill Factor. *PROGRESS IN PHOTOVOLTAICS: RESEARCH AND APPLICATIONS , 16*, 235-239.

Rogacheva, E. I., Tavrina, T. V., Nashchekina, O. N., Grigorov, S. N., Nasedkin, K. A., Dresselhaus, M. S. & Cronin, S. B. (2002). Quantum size effects in PbSe quantum wells. *APPLIED PHYSICS LETTERS , 15*, 2690-2691.

Romeo, A., Khrypunov, G., Galassini, S., Zogg, H., & Tiwari, A. (2007). Bifacial configurations for CdTe solar cells. *Solar Energy Materials & Solar Cells , 91*, pp.1388–1391.

Romeo, A., Khrypunov, G., Kurdesau, F., Arnold, M., Batzner, D., Zogg, H., & Tiwari, A. N. (2006). High-efficiency flexible CdTe solar cells on polymer substrates. *Solar Energy Materials & Solar Cells , 90*, pp. 3407–3415.

Romeo, A., Terheggen, M., Abou-Ras, D., Ba¨tzner, L. D., Haug, F.-J., Ka¨lin, M., Rudmann, D. & Tiwari, A. N. (2004). Development of Thin-film Cu(In,Ga)Se_2 and CdTe Solar Cells. *Prog. Photovolt: Res. Appl. , 12*, 93-111.

Romeo, N., Bosio, A., & Romeo, A. (2010). An innovative process suitable to produce high-efficiency CdTe/CdS thin-film modules. *Solar Energy Materials & Solar Cells , 94*, pp. 2–7.

Romeo, N., Bosio, A., Canevari, V., & Podesta, A. (2004). Recent progress on CdTe/CdS thin film solar cells. *Solar Energy , 77*, pp. 795–801.

Romeo, N., Bosio, A., Canevari, V., Terheggen, M., & Vaillant Roca, L. (2003). Comparison of different conducting oxides as substrates for CdS/CdTe thin film solar cells. *Thin Solid Films , 431-432*, pp.364–368.

Romeo, N., Bosio, A., Mazzamuto, S., Romeo, A., & Vaillant-Roca, L. (2007). A HIGH EFFICIENCY CdTe/CdS THIN FILM SOLAR CELLS WITH A NOVEL BACK-CONTACT. *22nd European Photovoltaic Solar Energy Conference*. Milan, Italy.

Rose, D. H., Hasoon, F. S., Dhere, R. G., Albin, D. S., Ribelin, R. M., Li, X., Yoxa Mahathongdy, S., Gessert, T. A. & Sheldon, P. (1999). Fabrication Procedures and Process Sensitivities for CdS/CdTe Solar Cells. *PROGRESS IN PHOTOVOLTAICS: RESEARCH AND APPLICATIONS , 7*, 331-340.

Sakurai, K., Hunger, R., Tsuchimochi, N., Baba, T., Matsubara, K., Fons, P., Yamada, A., Kojima, T., Deguchi, T., Nakanishi, H. & Niki, S. (2003). Properties of $CuInGaSe_2$ solar cells based upon an improved three-stage process. *Thin Solid Films , 431-432*, 6-10.

Santos-Cruz, J., Torres-Delgado, G., Castanedo-Perez, R., Jimenez-Sandoval, S., Marquez-Marın, J., & Zelaya-Angel, O. (2006). Au–Cu/p–CdTe/n–CdO/glass-type solar cells. *Solar Energy Materials & Solar Cells , 90*, pp. 2272–2279.

Sathiya Priya, A. R., Subramania, A., Jung, Y. S., & Kim, K. J. (2008). High-Performance Quasi-Solid-State Dye-Sensitized Solar Cell Based on an Electro spun PVdF-HFP Membrane Electrolyte. *Langmuir , 24*, 9816-9819.

Shafarman, W. N., & Stolt, L. (2003). Cu(InGa)Se_2 Solar Cells. In A. Luque, & S. Hegedus, *Handbook of Photovoltaic Science and Engineering*. John Wiley & Sons, Ltd.

Sharma, R. K., Jain, K., & Rastogi, A. C. (2003). Growth of CdS and CdTe thin films for the fabrication of n-CdS/p-CdTe solar cell. *Current Applied Physics , 3*, pp. 199–204.

Shirakata, S., Ohkubo, K., Ishii, Y., & Nakada, T. (2009). Effects of CdS buffer layers on photoluminescence properties of Cu(In,Ga)Se_2 solar cells. *Solar Energy Materials & Solar Cells , 93*, 988–992.

Singh, V. P., & McClure, J. C. (2003). Design issues in the fabrication of CdS–CdTe solar cells on molybdenum foil substrates. *Solar Energy Materials & Solar Cells , 76*, pp. 369–385.

Singh, V. P., McClure, J. C., Lush, G., Wang, W., Wang, X., Thompson, G., & Clark, E. (1999). Thin film CdTe-CdS heterojunction solar cells on lightweight metal substrates. *Solar Energy Materials & Solar Cells , 59*, pp. 145-161.

Stathatos, E., & Lianos, P. (2007). Increase of the Efficiency of Quasi-Solid State Dye-Sensitized Solar Cells by a Synergy between Titania Nanocrystallites of Two Distinct Nanoparticle Sizes. *Adv. Mater. , 19*, 3338-3341.

Sternitzke, M. (1997). Review: Structual Ceramic Nanocomposites. *Journal of the Europ-ean Ceramic , 17*, 1061-1082.

Tena-Zaera, R., Katty, A., Bastide, S., Levy-Clement, C., ORegan, B., & Munoz-Sanjose, V. (2005). ZnO/CdTe/CuSCN, a promising heterostructure to act as inorganic eta-solar cell. *Thin Solid Films , 483*, 372-377.

Thampi, K., Bessho, T., Gao, F., Zakeeruddin, S., Wan, P. & Grätzel, M. (2008). New materials improve dye sensitized solar cell performance. *23rd European Photovoltaic Solar Energy Conference and Exhibition*, (pp. 153-155). Valencia, Spain.

Tiwari, A. N., Khrypunov, G., Kurdzesau, F., Batzner, D. L., Romeo, A., & Zogg, H. (2004). CdTe Solar Cell in a Novel Configuration. *Prog. Photovolt: Res. Appl. , 12*, pp. 33–38.

Tjong, S. (2006). Structural and mechanical properties of polymer nanocomposites. *Materials Science and Engineering , R* (53), 73-197.

Tokita, Y., Chaisitsak, S., Yamada, A. & Konagai, M. (2003). High-efficiency Cu(In,Ga)Se_2 thin-film solar cells with a novel $In(OH)_3$:Zn^{2+} buffer layer. *Solar Energy Materials & Solar Cells , 75*, 9-15.

Tsuji, M., Aramoto, T., Ohyama, H., Hibino, T. & Omura, K. (2000). Characterization of CdS thin film in high efficient CdS/CdTe solar cells. *Journal of Crystal Growth , 214/215*, pp. 1142-1147.

Ullal, H. & Roedern, B. v. (2007). Thin Film CIGS and CdTe Photovoltaic Technologies: Commercialization, Critical Issues, and Applications. *the 22nd European Photovoltaic Solar Energy Conference (PVSEC) and Exhibition*. Milan, Italy.

Vigil-Galán, O., Sánchez-Meza, E., Ruiz, C., Sastré-Hernández, J., Morales-Acevedo, A., Cruz- Gandarilla, F., Aguilar-Hernández, J., Saucedo, E., Contreras-Puente, G. & Bermúdez, V. (2007). Physical properties of Bi doped CdTe thin films grown by CSVT and their influence on the CdS/CdTe solar cells PV-properties. *Thin Solid Films , 515*, 5819–5823.

Wang, P., Zakeeruddin, S. M., Moser, J. E., Humphry-Baker, R., Comte, P., Aranyos, V., Hagfeldt, A., Nazeeruddin, M. K. & Grätzel, M. (2004). Stable New Sensitizer with Improved Light Harvesting for Nanocrystalline Dye-Sensitized Solar Cells. *Adv. mater. , 16* (20), 1806-1811.

Wu, J., Lan, Z., Hao, S., Li, P., Lin, J., Huang, M., Fang,L & Huang, Y. (2008). Progress on the electrolytes for dye-sensitized solar cells. *Pure Appl. Chem. , 80* (11), 2241-2258.

Wu, X. (2004). High-efficiency polycrystalline CdTe thin-film solar cells. *Solar Energy , 77*, pp. 803–814.

Wu, X., Dhere, R. G., Albin, D. S., Gessert, T. A., DeHart, C., Keane, J. C., Duda, A., Coutts,T.J., Asher, S., Levi, D. H., Moutinho, H. R., Yan, Y., Moriarty, T., Johnston, S., Emery, K. & Sheldon, P. (2001). High-Efficiency CTO/ZTO/CdS/CdTe Polycrystalline Thin-Film Solar Cells. *NCPV Program Review Meeting*. Lakewood, Colorado.

Wu, X., Sheldon, P., Mahathongdy, Y., Ribelin, R., Mason, A., Moutinho, H.R. & Coutts, T. J. (1998). CdS/CdTe Thin-Film Solar Cell with a Zinc Stannate Buffer Layer. *National Renewable Energy Laboratory Presented at the National Center for Photovolt Program Review meeting*. Denver, Colorado.

Wu, X., Zhou, J., Duda, A., Keane, J. C., Gessert, T. A., Yan, Y. & Noufi, R. (2006). 13.9%-efficient CdTe Polycrystalline Thin-film Solar Cells with an Infrared Transmission of ~50%. *Prog. Photovolt: Res. Appl. , 14*, pp. 471–483.

Wu, X., Zhou, J., Keane, J., Dhere, R., Albin, D. S., Gessert, T.A., DeHart, C., Duda, A.,Ward, J. J., Yan, Y., Teeter, G., Levi, D. H., Asher, S., Perkins, C., Moutinno, H. R., To, B., Emery, K., Moriarty, T., Zhang, Y., Wei, S., Coutts, T.& Noufi, R. (2005). Advances in CdTe R&D at NREL. *the 2005 DOE Solar Energy Technologies Program Review Meeting*. Denver, Colorado.

Wuerz, R., Eicke, A., Frankenfeld, M., Kessler, F., Powalla, M., Rogin, P. & Yazdani-Assl, O (2009). CIGS thin-film solar cells on steel substrates. *Thin Solid Films , 517*, pp. 2415–2418.

Yanagida, M., Onozawa-Komatsuzaki, N., Kurashige, M., Sayama, K., & Sugihara, H. (2010). Optimization of tandem-structured dye-sensitized solar cell. *Solar Energy Materials & Solar Cells , 94*, 297-302.

Ying, D., & Zhang, D. (2000). Processing of Cu–Al_2O_3 metal matrix nanocomposite materials by using high energy ball milling. *Materials Science and Engineering , A286*, 152–156.

Yongbai, Y. (2007). Nanocomposite thin films for solar energy conversion. In S. Zhang, & N. Ali, *Nanocomposite thin films and coatings Processing, Properties and Performance* (pp. 381-417). Imperial College Press.

Yoon, C. H., Vittal, R., Lee, J., Chaec, W.-S., & Kima, K.-J. (2008). Enhanced performance of a dye-sensitized solar cell with an electrodeposited-platinum counter electrode. *Electrochimica Acta , 53*, 2890–2896.

Zhang, G., Bala, H., Cheng, Y., Shi, D., Lv, X., & Yu, Q. &. (2009). High efficiency and stable dye-sensitized solar cells with an organic chromophore featuring a binary π-conjugated spacer. *Chem. Commun.* , 2198-2200.

Zhang, N., Zhuang, D.-M., & Zhang, G. (2010). An investigation on preparation of CIGS targets by sintering process. *Materials Science and Engineering B , 166*, pp. 34–40.

Zhang, R., Pan, J., Briggs, E. P., Thrash, M., & Kerr, L. L. (2008). Studies on the adsorption of RuN3 dye on sheet-like nanostructured porous ZnO films. *Solar Energy Materials & Solar Cells , 92*, 425-431.

Zhao, Q., Liu, C., Liu, H., Zhang, L., & Yao, X. (1994). Quantum size effects and nonlinear optical properties of ZnS and CdS semiconductor-doped silica glasses prepared by

sol-gel process. *Applications of Ferroelectrics, 1994 .ISAF '94., Proceedings of the Ninth IEEE International Symposium on*, (pp. 797-800). University Park, PA.

Zoppi, G., Durose, K., Irvine, S. J., & Barrioz, V. (2006). Grain and crystal texture properties of absorber layers in MOCVD-grown CdTe/CdS solar cells. *Semicond. Sci. Technol. , 21*, 763-770.

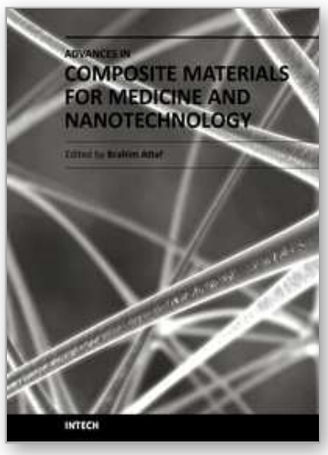

Advances in Composite Materials for Medicine and Nanotechnology

Edited by Dr. Brahim Attaf

ISBN 978-953-307-235-7
Hard cover, 648 pages
Publisher InTech
Published online 01, April, 2011
Published in print edition April, 2011

Due to their good mechanical characteristics in terms of stiffness and strength coupled with mass-saving advantage and other attractive physico-chemical properties, composite materials are successfully used in medicine and nanotechnology fields. To this end, the chapters composing the book have been divided into the following sections: medicine, dental and pharmaceutical applications; nanocomposites for energy efficiency; characterization and fabrication, all of which provide an invaluable overview of this fascinating subject area. The book presents, in addition, some studies carried out in orthopedic and stomatological applications and others aiming to design and produce new devices using the latest advances in nanotechnology. This wide variety of theoretical, numerical and experimental results can help specialists involved in these disciplines to enhance competitiveness and innovation.

InTech Europe
University Campus STeP Ri
Slavka Krautzeka 83/A
51000 Rijeka, Croatia
Phone: +385 (51) 770 447
Fax: +385 (51) 686 166
www.intechopen.com

InTech China
Unit 405, Office Block, Hotel Equatorial Shanghai
No.65, Yan An Road (West), Shanghai, 200040, China
中国上海市延安西路65号上海国际贵都大饭店办公楼405单元
Phone: +86-21-62489820
Fax: +86-21-62489821

IntechOpen